bioRxiv preprint doi: https://doi.org/10.1101/348797; this version posted June 15, 2018. The copyright holder for this preprint (which was not certified by peer review) is the author/funder, who has granted bioRxiv a license to display the preprint in perpetuity. It is made available under aCC-BY 4.0 International license.

Regulation of the Unfolded Protein Response by BiP AMPylation protects photoreceptors from light-dependent degeneration.

Andrew T. Moehlman[1], Amanda K. Casey[2], Kelly Servage[2,3], Kim Orth[2,3*], Helmut Krämer[1,4*]

Affiliations:

[1]Department of Neuroscience, UT Southwestern Medical Center, Dallas, TX.

[2]Department of Molecular Biology UT Southwestern Medical Center, Dallas, TX.

[3]Department of Biochemistry, UT Southwestern Medical Center, Dallas, TX and Howard Hughes Medical Institute, Dallas, TX.

[4]Department of Cell Biology, UT Southwestern Medical Center, Dallas, TX.

*Correspondence to:

Helmut.Kramer@UTSouthwestern.edu,

Kim.Orth@utsouthwestern.edu

bioRxiv preprint doi: https://doi.org/10.1101/348797; this version posted June 15, 2018. The copyright holder for this preprint (which was not certified by peer review) is the author/funder, who has granted bioRxiv a license to display the preprint in perpetuity. It is made available under aCC-BY 4.0 International license.

Abstract

In response to environmental, developmental, and pathological stressors, cells engage homeostatic pathways to maintain their function. Among these pathways, the Unfolded Protein Response protects cells from the accumulation of misfolded proteins in the ER. Depending on ER stress levels, the ER-resident Fic protein catalyzes AMPylation or de-AMPylation of BiP, the major ER chaperone and regulator of the Unfolded Protein Response. This work elucidates the importance of the reversible AMPylation of BiP in maintaining the *Drosophila* visual system in response to stress. After 72 hours of constant light, photoreceptors of *fic*-null and AMPylation-resistant BiP^{T366A} mutants, but not wild-type flies, display loss of synaptic function, disintegration of rhabdomeres, and excessive activation of ER stress reporters. Strikingly, this phenotype is reversible: photoreceptors regain their structure and function within 72 hours once returned to a standard light:dark cycle. These findings show that Fic-mediated AMPylation of BiP is required for neurons to adapt to transient stress demands.

Introduction

Post-translational modifications (PTMs) of proteins are important for rapid responses to environmental challenges of cells. One such PTM is AMPylation, the reversible addition of adenosine monophosphate (AMP) to hydroxyl groups (also known as adenylylation) (Brown et al., 1971; Casey & Orth, 2018; Kingdon et al., 1967; Woolery et al.). AMPylation is catalyzed by at least two protein families, among them the conserved Fic-domain proteins (Casey & Orth, 2018; Harms et al., 2016). Eukaryotic Fic, an ER-resident type-II membrane protein (Rahman et al., 2012), AMPylates BiP (GRP78), a highly conserved and ubiquitous ER chaperone (Ham et

bioRxiv preprint doi: https://doi.org/10.1101/348797; this version posted June 15, 2018. The copyright holder for this preprint (which was not certified by peer review) is the author/funder, who has granted bioRxiv a license to display the preprint in perpetuity. It is made available under aCC-BY 4.0 International license.

al., 2014; Preissler et al., 2015). Working together with a multitude of associated quality control proteins, BiP is critical for the translocation, folding, and secretion of proteins from the ER as well as for aiding in the clearing of misfolded ER aggregates and degradation of membrane-associated proteins (Hendershot et al., 1988; Kozutsumi et al., 1988; Meunier et al., 2002). BiP is both a mediator and transcriptional target of the Unfolded Protein Response (UPR), a coordinated cell signaling pathway that is activated during times of high misfolded protein levels in the ER. Like many protein chaperones, BiP depends on its ATPase activity to undergo a conformational change to bind to its substrates (Gaut & Hendershot, 1993). AMPylation locks BiP into a state resembling the ATP-bound conformation with high substrate off-rates, thereby inhibiting its chaperone function (Preissler, Rohland, et al., 2017; Wieteska et al., 2017).

In agreement with this PTM's inhibitory role, BiP AMPylation levels are linked to protein homeostasis (Ham et al., 2014). Reduction of ER protein load promotes Fic-mediated AMPylation of BiP, whereas Fic catalyzes the deAMPylation of BiP under elevated ER stress conditions (Ham et al., 2014; Preissler et al., 2015). This switch in Fic's activity is linked to a key regulatory salt bridge in eukaryotic Fic. Mutations in Fic that disrupt this salt bridge result in an overactive AMPylator that lacks deAMPylation activity (Casey et al., 2017; Preissler, Rato, et al., 2017). Together, these studies suggest a model in which BiP is AMPylated in times of low ER stress, creating a reserve pool of inactive BiP that can be readily activated to respond to changes of ER homeostasis (**Figure 1A**). This reserve pool of BiP is proposed to act as a buffer to attenuate or shorten the need for a more dramatic activation of the transcriptional and translational arms of the UPR (Casey et al., 2017; Preissler, Rato, et al., 2017; Wieteska et al., 2017). However, the physiological importance of endogenous Fic-mediated AMPylation for remains unclear.

bioRxiv preprint doi: https://doi.org/10.1101/348797; this version posted June 15, 2018. The copyright holder for this preprint (which was not certified by peer review) is the author/funder, who has granted bioRxiv a license to display the preprint in perpetuity. It is made available under aCC-BY 4.0 International license.

In the fruit fly, *Drosophila melanogaster*, we previously demonstrated that *fic*-null mutants harbor a defect in visual signaling, as assessed by electroretinogram (ERG). The well-characterized Drosophila visual system has proven a valuable model for many fields, such as neuroscience (Borycz et al., 2002; Sugie et al., 2015), cell signaling (Dolph et al., 1993; Scott et al., 1995), protein trafficking (Akbar et al., 2009; Lee et al., 2003), and neurodegeneration (Johnson et al., 2002; Leonard et al., 1992; Ryoo et al., 2007). The specialized photoreceptor cells possess tightly packed microvilli-like membranes, termed rhabdomeres, that endow remarkable sensitivity to minute changes in light conditions (Montell, 2012). The ability to maintain this sensitivity is critical for flight behavior, foraging, and escape from predators. Thus, under a wide range of conditions, photoreceptors must maintain their light detection cascade, which requires the constant production, trafficking, and degradation of proteins through the endomembrane system (Colley et al., 1995; Kiselev et al., 2000; Rosenbaum et al., 2006).

We postulated that as a regulator of proteostasis and the UPR, BiP must be tightly regulated for proper maintenance of vision in the fly. Here we demonstrate that mutants lacking AMPylation of BiP at a specific residue, Thr366, possess the same ERG defect as *fic*-null animals, implicating BiP as the target of Fic necessary for visual signaling. We go on to find that application of an eye-specific stress, constant light, leads to exaggerated electrophysiology defects and the loss of photoreceptor rhabdomeres, akin to neurodegeneration. However, these defects exhibit a remarkable and unique reversibility: structural and functional phenotypes observed in light-stressed *fic*-null and AMPylation-resistant BiP^{T366A} mutants are reversed after the flies are returned to a standard light/dark cycle. In addition, we identify changes in the regulation of UPR during constant light stress in these mutants, implicating ER dysregulation as the cause of the inability to adapt to altered light conditions.

bioRxiv preprint doi: https://doi.org/10.1101/348797; this version posted June 15, 2018. The copyright holder for this preprint (which was not certified by peer review) is the author/funder, who has granted bioRxiv a license to display the preprint in perpetuity. It is made available under aCC-BY 4.0 International license.

Results

BiP^{T366A} rescues over-expression of constitutively active AMPylating Fic^{E247G}

To test the hypothesis that BiP is a critical target of Fic AMPylation *in vivo* (**Figure 1A**), we designed and generated transgenes expressing wild-type and AMPylation-resistant FLAG-tagged BiP proteins under control of the endogenous BiP promoter (**Figure 1- figure supplement 1A**). *BiP* null fly mutants die early in development; this lethality is rescued by including a copy of the genomic transgene expressing FLAG-BiP^{WT} or the AMPylation-resistant FLAG-BiP^{T366A} mutant (**Figure 1B**). We will refer to these rescued flies as *BiP*^{WT} or *BiP*^{T366A}, respectively. In contrast, a BiP transgene mutated at a second reported AMPylation site (Casey et al., 2017; Preissler et al., 2015), BiP^{T518A}, did not rescue *BiP*$^{-/-}$ lethality. As *fic* null mutants that lack BiP AMPylation are viable, the lethality of the *BiP*^{T518A} mutant is not likely to be due to the loss of AMPylation (Casey et al., 2017). Instead, these observations indicate an essential role for Thr^{518} in BiP's chaperone activity. Consistent with this notion, the equivalent residue, Thr^{538}, in the *S. cerevisiae* BiP homolog Kar2 is required for survival under heat stress even though yeast lack both Fic domain proteins and BiP AMPylation (**Figure 1- figure supplement 1B**).

Previously, we reported that over-expression of the constitutively active AMPylating Fic^{E247G} was lethal in a *fic*-null fly background (*fic*^{30C}) because it lacks the essential deAMPylation activity (Casey et al., 2017). We tested whether flies expressing the AMPylation-resistant BiP^{T366A} could survive this lethality. Consistent with previous findings, we observe over-expression of the mutant UAS-Fic^{E247G} transgene using the ubiquitous *Da*-Gal4 driver was lethal in an otherwise *fic*-null animal (**Figure 1C**). Lethality of the constitutively active AMPylating Fic^{E247G} was suppressed in flies expressing the AMPylation-resistant BiP^{T366A} but

bioRxiv preprint doi: https://doi.org/10.1101/348797; this version posted June 15, 2018. The copyright holder for this preprint (which was not certified by peer review) is the author/funder, who has granted bioRxiv a license to display the preprint in perpetuity. It is made available under aCC-BY 4.0 International license.

not BiP^{WT} (**Figure 1C**). These results indicate that Thr^{366} of BiP is a physiologically relevant AMPylation target *in vivo*.

The UPR protects eyes from overactive AMPylation

To test the interaction between Fic-mediated AMPylation and the UPR, we employed an eye-specific Fic gain-of-function model. Eye-specific expression of the constitutively active AMPylating UAS-Fic^{E247G} transgene using a LongGMR-Gal4 driver in otherwise *fic*-null animals results in a severe rough-eye defect (Casey et al., 2017). However, in a *fic* heterozygous background, eye-specific expression of constitutively active AMPylating Fic^{E247G} yields only a mildly rough eye (**Figure 2A**). We used this intermediate phenotype to assess genetic interactions between Fic^{E247G} and components of the UPR with a candidate-based targeted RNAi screen (**Table 1**). Fic^{E247G}-induced eye roughness was significantly enhanced by knockdown of the key UPR components *Perk*, *Atf4*, and *Ire1* (**Figure 2C-E** and **Table 1**), but not *ATF6* **(Figure 2B)**. Furthermore, *Xbp1* knockdown in conjunction with Fic^{E247G} expression was lethal (**Figure 2F**). By contrast, knockdown of these UPR genes in in the absence of Fic^{E247G} did not influence eye phenotype or fly survival (**Figure 2A'-F').** These genetic interactions suggest a role for UPR signaling in mitigating cellular stress imposed by expressing the constitutively active AMPylating Fic^{E247G} in the eye.

AMPylation of BiP is necessary for maintaining vision

The findings that BiP is a target of Fic *in vivo* and that silencing UPR pathway components enhances the severity of the constitutively active AMPylating Fic^{E247G}-induced rough-eye phenotype prompted us to assay the physiological effects of cellular stress in flies

bioRxiv preprint doi: https://doi.org/10.1101/348797; this version posted June 15, 2018. The copyright holder for this preprint (which was not certified by peer review) is the author/funder, who has granted bioRxiv a license to display the preprint in perpetuity. It is made available under aCC-BY 4.0 International license.

lacking BiP AMPylation. To do this we utilized flies that are either null for *fic* (fic^{30C}) or express the AMPylation-resistant BiP^{T366A} instead of wild-type BiP. By using this strategy, we are able to discern BiP AMPylation-specific changes from other potential changes that are due to as-yet-unknown targets of Fic AMPylation.

As previously reported in ERG recordings, *fic*-null flies display a reduction of the initial response (termed the ON Transient, Figure 3A) to a light pulse compared to wild-type controls. Interestingly, BiP^{T366A}, but not BiP^{WT} flies, exhibited the same defect in ON Transients as fic^{30C} mutants, consistent with BiP being the primary target of Fic AMPylation required for proper visual neurotransmission (**Figure 1- figure supplement 2**). Of note, we used an eye-specific RNAi construct against *white* to minimize any effect of the *mini-white* gene used as a marker in these BiP transgenes. When we compared ERG traces of fic^{30C} and BiP^{T366A} flies in *white*+ (red eyed) backgrounds, the reductions in ON transients were no longer detectable (**Figure 1- figure supplement 3**). This is likely due to the previously established protective effect provided by the red pigment in $white^{+}$ flies. Indeed, a similar *white*-dependent phenotype has been reported for photoreceptor synaptic plasticity after prolonged light exposure (Damulewicz et al., 2017; Sugie et al., 2015), consistent with previous observations that a functional *white* gene masks some degenerative phenotypes in the retina (Lee & Montell, 2004; Soukup et al., 2013). Therefore, we used the *white*-eyed flies (referred to as w^{1118}) to test whether AMPylation may play a role in this type of photoreceptor plasticity, which is induced by rearing flies in uninterrupted low light for 72 hours (Damulewicz et al., 2017; Sugie et al., 2015).

We conducted ERG recordings under different light conditions with four fly lines, w^{1118}, fic^{30C}, BiP^{WT} and BiP^{T366A} (**Figure 3B**). Compared to age-matched siblings reared under the standard 12 hr Light:12 hr Dark (LD) treatment, fic^{30C} and BiP^{T366A} flies reared for three days

bioRxiv preprint doi: https://doi.org/10.1101/348797; this version posted June 15, 2018. The copyright holder for this preprint (which was not certified by peer review) is the author/funder, who has granted bioRxiv a license to display the preprint in perpetuity. It is made available under aCC-BY 4.0 International license.

under continuous light (LL) at 500 lux exhibited severe ERG defects. This included reduction in the sustained negative potential (SNP), a measure of photoreceptor activation, and loss of ON and OFF transients, which reflect synaptic transmission to downstream L1/L2 lamina neurons (**Figure 3C & D**). Wild-type controls maintained healthy OFF transients following LL, but ON transients were reduced, reflecting the sensitivity of this component to various light conditions (**Figure 3D**). To test for behavioral consequences, we assayed w^{1118} and fic^{30C} flies after 72 hours of LD or LL treatment for light-induced startle behavior using single-fly activity chambers (Ni et al., 2017). Following a 5-min light pulse, LD-reared fic^{30C} flies exhibited a startle response indistinguishable from control w^{1118} flies, whereas fic^{30C} flies, but not w^{1118} flies, failed to respond to the light pulse after 72 hours of LL (**Figure 3- figure supplement 1**). Thus, Fic-mediated AMPylation is required to maintain vision acuity under LL conditions.

We next designed experiments to test whether these functional ERG changes in flies lacking AMPylation reflected light-induced neurodegeneration or a failure to adapt to constant stimulation. First, we asked if the LL-induced ERG defects of BiP^{T366A} and fic^{30C} flies were reversible. We reared mutant and control flies for 72 hours in LL followed by 72 hours of recovery in LD (referred to as "Rec"; **Figure 3B**). This recovery period was sufficient to restore both healthy OFF transients and SNPs in BiP^{T366A} and fic^{30C} flies **(Figure 3C & D)**. Second, we asked if the intensity of the light would exaggerate the defects of BiP^{T366A} and fic^{30C} flies. Exposure of mutant or control flies with 5000 lux, instead of 500 lux, did not alter the severity of ERG defects, indicating the changes were not simply a reflection of the increased amount of total light exposure during LL treatment (**Figure 3- figure supplement 2**). Third, we asked if prolonging the LL stress would alter the reversibility of these defects. Mutant flies reared under LL for ten days retained the capability to recover healthy ERG traces after only three days on

bioRxiv preprint doi: https://doi.org/10.1101/348797; this version posted June 15, 2018. The copyright holder for this preprint (which was not certified by peer review) is the author/funder, who has granted bioRxiv a license to display the preprint in perpetuity. It is made available under aCC-BY 4.0 International license.

LD, indicating that photoreceptors are not dying but maintained during prolonged light stress (**Figure 3- figure supplement 3**). Together, these data support a model for a dysregulated adaptive response, rather than phototoxicity, inducing the reversible loss of OFF transients and reduced SNPs.

Constant light induces severe but reversible morphological defects in AMPylation mutants

To determine if the underlying eye substructures were being altered in these AMPylation deficient mutants, we performed TEM on ultrathin transverse eye sections. Under LD conditions, *fic*^{30C} and *BiP*^{T366A} mutant and wild-type controls appeared indistinguishable (**Figure 4A**). However, following 72 hours of LL (500 lux), *fic*^{30C} and *BiP*^{T366A} mutants, but not w^{1118} and *BiP*^{WT} controls, displayed severe defects in the integrity of rhabdomeres, the microvilli-like membrane structures that house the phototransduction cascade (**Figure 4B**). After a three-day recovery at LD, the rhabdomeres were nearly restored in both AMPylation-deficient mutants (**Figure 4C**). To quantify these structural changes in large cohorts of flies, we assessed flies for the presence of wild-type "deep pseudopupils" (DPP) (**Figure 4D**). Visualization of the DPP affords an assessment of rhabdomere structural integrity in living flies (Franceschini & Kirschfeld, 1971). Consistent with the TEM data, 3 days of LL caused loss of DPP in *fic*^{30C} and *BiP*^{T366A}, and DPPs returned after a 3-day recovery (**Figure 4D**). This suggests that proper regulation of BiP through AMPylation is required for maintaining both function and structure of photoreceptor cells.

bioRxiv preprint doi: https://doi.org/10.1101/348797; this version posted June 15, 2018. The copyright holder for this preprint (which was not certified by peer review) is the author/funder, who has granted bioRxiv a license to display the preprint in perpetuity. It is made available under aCC-BY 4.0 International license.

Fic regulates ER stress signaling in the retina and lamina neuropil

Given the unique role of Fic in both AMPylating and deAMPylating BiP to modulate its chaperone activity and maintaining ER homeostasis, we evaluated *fic*^{30C} flies for changes in the UPR under LD, LL, and Rec conditions. First, we performed immunohistochemistry against BiP, a transcriptional target of the UPR, which is upregulated during states of ER stress (Gardner et al., 2013; Ham et al., 2014). After 3 days of LL, sections of *fic*^{30C} revealed increased levels of BiP in retinas and in the lamina neuropils where photoreceptor axons form synapses onto lamina neurons. BiP levels returned to control levels following three days of recovery (**Figure 5A & B**). To further assess UPR signaling in these tissues, we utilized a sensor for Ire1-mediated Xbp1 splicing (Sone et al., 2013) and an Atf4 translational reporter which serves as a proxy for Perk-mediated phosphorylation of eIF-2a (Kang et al., 2015). In wild-type flies, Xbp1-GFP was slightly induced in the lamina after 24 hours of LL in wild-type flies and the signal decreased over time (**Figure 5C, top row, & 5D**). However, in *fic*^{30C} flies, the Xbp1-GFP signal in the lamina continued to increase after 48 hours of LL and remained elevated after 72 hours (**Figure bottom row, & 5D).** In the retina, control flies showed little to no increase of Xbp1-GFP levels, while *fic*^{30C} flies showed a significant transient increase after one and two days LL. With the Atf4-DsRed reporter, we observed a significant increase of signal in both the retina and lamina of wild-type flies after one day, but no difference in *fic*^{30C} mutants at one or two days LL when compared to LD controls (**Figure 5E & F**). However, by three days of LL, Atf4-DsRed reporter activity in the wild-type flies returned to control levels, while the *fic*^{30C} mutants showed a significant increase in both the retina and lamina neuropil (**Figure 5E & F**). These changes in UPR signaling were reversible as each of the reporters returned to near control intensity after 72 hours of LD recovery (**Figure 5A, C & E, last columns**). The elevated UPR response in

bioRxiv preprint doi: https://doi.org/10.1101/348797; this version posted June 15, 2018. The copyright holder for this preprint (which was not certified by peer review) is the author/funder, who has granted bioRxiv a license to display the preprint in perpetuity. It is made available under aCC-BY 4.0 International license.

224 *fic*^{30C} mutants correlated with the timing of the observed severe defects in the integrity of
225 rhabdomeres (**Figure 4B**). Together, these data identify a crucial role for Fic-mediated BiP
226 AMPylation in regulating UPR signaling during homeostatic responses of photoreceptor
227 neurons.
228

229 **Discussion**

230 Here we demonstrate that BiP is a critical *in-vivo* target of Fic-mediated AMPylation, as
231 an AMPylation-resistant BiP blocks over-expressed constitutively active AMPylating Fic^{E247G}
232 lethality and recapitulates *fic*-null vision defects. This work also sheds light on a novel
233 physiological role for AMPylation/deAMPylation control of BiP: fine-tuning UPR signaling to
234 allow for visual system adaptation. We observe genetic interactions with the constitutively active
235 AMPylating Fic^{E247G} and the UPR sensors Ire1 and PERK as well as their effectors, perhaps due
236 to the critical role of BiP as both a regulator (Amin-Wetzel et al., 2017; Bertolotti et al., 2000;
237 Carrara et al., 2015; Shen et al., 2005) and downstream transcriptional target of the UPR (Ham et
238 al., 2014; Kozutsumi et al., 1988). Indeed, we hypothesize that unregulated Fic^{E247G}, in the
239 absence of deAMPylation activity, AMPylates excess BiP, excluding it from its normal
240 chaperone role and leading to cell death (Casey et al., 2017; Truttmann et al., 2017). In support
241 of this hypothesis, the developmental defects due to excessive unregulated AMPylation are
242 suppressed by AMPylation-resistant BiP^{T366A}. Furthermore, the enhancement of the rough-eye
243 Fic^{E247G} phenotype by knockdown of the Ire1 and PERK pathways suggest a protective role for
244 the UPR, perhaps through the known effects on translation by Ire1-mediated decay of mRNA,
245 Xbp1-driven transcription or PERK-mediated phosphorylation of eIF-2a (Gardner et al., 2013).

bioRxiv preprint doi: https://doi.org/10.1101/348797; this version posted June 15, 2018. The copyright holder for this preprint (which was not certified by peer review) is the author/funder, who has granted bioRxiv a license to display the preprint in perpetuity. It is made available under aCC-BY 4.0 International license.

Our work supports an *in-vivo* requirement for Fic-mediated AMPylation of BiP^{T366} in the context of long-term adaptation to prolonged light exposure. BiP^{T366} replacement mutants phenocopy *fic*-null flies in both the light-induced blindness and the unexpected recovery from this phenotype. These functional changes are mirrored in the structural changes of photoreceptor rhabdomeres. Rhabdomere appearance of AMPylation deficient flies was reminiscent of retinal degeneration mutants (Ryoo et al.; Smith et al., 1991), however the remarkable recovery of the tissue structure in three days is unlike any reported retinal degeneration phenotype. Together, this work demonstrates a seminal role for Fic-mediated AMPylation of BiP *in vivo*: enabling photoreceptors to adapt and maintain both structural and functionality integrity during periods of prolonged stress due to uninterrupted light stimulation. The exact mechanism through which these defects in *fic* mutants arise remains undetermined, but previous studies have demonstrated a requirement for maintaining normal ER folding and trafficking of transmembrane visual signaling components, such as Rhodoposin (Colley et al., 1995; Rosenbaum et al., 2006). This intense demand for proper ER stress regulation sensitizes the eye to otherwise mild defects in *fic* mutants, and the additional demands posed by the stress of constant light stimulation.

We also observed that loss of BiP AMPylation deregulates, but does not block, the UPR to this physiological stress. This observation supports previous claims that AMPylation and deAMPylation of BiP aids in maintaining ER homeostasis (**Figure 1A**) by establishing a reserve pool of BiP that can readily be deAMPylated in response to acute ER insults (Casey et al., 2017; Ham et al., 2014; Preissler, Rato, et al., 2017). This regulation would allow for fine-tuning of the UPR response under specific contexts, comparable to findings in *C. elegans* in which *fic-1* and *hsp3* (a BiP homologue) mutants are sensitive to bacterial infection (Truttmann et al., 2016). We speculate that the eye requires tight control of BiP activity and suppression of UPR signaling, to

bioRxiv preprint doi: https://doi.org/10.1101/348797; this version posted June 15, 2018. The copyright holder for this preprint (which was not certified by peer review) is the author/funder, who has granted bioRxiv a license to display the preprint in perpetuity. It is made available under aCC-BY 4.0 International license.

facilitate adaptation of the vision signaling cascade. Under standard LD conditions, only slight differences are observed, presumably because ER stress is low (**Figure 5C & D**, **1st column**). However, exposure to constant light results in ER stress and UPR signaling, which wild-type flies can clear, presumably because there is a reserve pool of AMPylated BiP to rapidly respond to the stress. In *fic* mutants, we speculate, loss of the reserve BiP results in the UPR dysregulation revealed by the IreI and PERK activity reporters (**Figure 5C & D**) as a larger proportion of BiP would be previously engaged and not able to respond to the extra stress. Additionally, the prolonged UPR response in the eyes with dysregulated AMPylation may result in increased expression of UPR-regulated proteins while blocking production of the visual signaling components necessary for adapting to transient stress.

BiP expression is subject to multiple levels of feedback regulation and is induced when the UPR is activated (Kozutsumi et al., 1988; Ma & Hendershot, 2003). However, in a negative feedback loop, BiP also inhibits activation of the UPR sensors Ire1, PERK, and Atf6, through direct binding (Bertolotti et al., 2000; Shen et al., 2005). It remains unknown how AMPylation affects the interactions of BiP with these proteins *in vivo*; however, *in-vitro* work suggests that AMPylation of BiP abolishes its inhibitory effect on Ire1 dimerization and activation (Amin-Wetzel et al., 2017). We speculate that the loss of BiP AMPylation/deAMPylation cycle in a *fic* null affects both the ability of BiP to quickly respond to misfolded protein aggregates and to regulate UPR activation. Future studies on the dynamic role of reversible BiP AMPylation and its interaction with downstream UPR sensors should provide unique insight into neuronal plasticity and regeneration.

bioRxiv preprint doi: https://doi.org/10.1101/348797; this version posted June 15, 2018. The copyright holder for this preprint (which was not certified by peer review) is the author/funder, who has granted bioRxiv a license to display the preprint in perpetuity. It is made available under aCC-BY 4.0 International license.

Materials and Methods

Fly stocks and genetics

Bloomington Stock Center provided w^{1118} (BS# 3605), *BiP*^{G0102}*/FM7c* (BS#11815), *Da*-Gal4 (BS#55850), *LongGMR*-Gal4 (*BS#8121*) stocks. The *fic*^{30C} allele and UAS-Fic^{E247G} flies was previously described (Casey et al., 2017). Lines used in the RNAi screen are described in Table S1 and were obtained from Bloomington Stock Center and the Vienna Drosophila Resource Center (Dietzl et al., 2007). The Atf4$^{5'UTR}$-dsRed (Kang et al., 2015) and the Xbp1-GFP (Sone et al., 2013) lines were a gift from Dr. Don Ryoo (NYU) and were recombined with the *fic*^{30C} allele. We generated the p[gen3xFLAG-BiP^{WT}]$^{AttP-89E11}$, p[gen3xFLAG-BiP^{T366A}]$^{AttP-89E11}$, p[gen3xFLAG-BiP^{T518A}]$^{AttP-89E11}$ and p[*GMR*-dsRNA^{white}] alleles using the Phi30C integrase strategy (Venken et al., 2006). p[*GMR*-dsRNA^{white}] was recombined with the *fic*^{30C} allele and white-eyed candidates were screened for the *fic* allele by PCR. *BiP*^{G0102};; p[gen3xFLAG-BiP^{WT}]$^{AttP-89E11}$ and *BiP*^{G0102};;p[gen3xFLAG-BiP^{T366A}]$^{AttP-89E11}$ stocks were made by crossing males harboring the genomic transgene to *BiP*^{G0102}/FM7c female flies. Surviving males were backcrossed to *BiP*^{G0102}/FM7c female flies, and stable stocks were established from the resulting progeny. None of the rare escaping *BiP*^{G0102} ;; p[gen3xFLAG-BiP^{T518A}]$^{AttP-89E11}$ male flies were fertile. The *LongGMR*-Gal4,UAS^{Scer}-V5-Fic^{E247G}-$^{attP-B3}$/TM6B,Hu and *Da*-Gal4,UAS^{Scer}-V5-Fic^{E247G}-$^{attP-B3}$/TM6B,hu stocks were made using standard Drosophila recombination and crossed into w^{1118} and w^{1118} *; fic*^{30C} backgrounds.

List of flies strains and stocks used

w^{1118} (BS#3605)

OreR

bioRxiv preprint doi: https://doi.org/10.1101/348797; this version posted June 15, 2018. The copyright holder for this preprint (which was not certified by peer review) is the author/funder, who has granted bioRxiv a license to display the preprint in perpetuity. It is made available under aCC-BY 4.0 International license.

314 ; *fic*^{30C}

315 w^{1118} ; *fic*^{30C}

316 w^{1118} ; p[*GMR*-dsRNA^{white}]

317 w^{1118} ; *fic*^{30C} , p[*GMR*-dsRNA^{white}]

318 w^{1118} ; *fic*^{30C} ; *LongGMR*-Gal4,UAS^{Scer}-V5-Fic^{E247G}- $^{attP-B3}$/TM6B,hu

319 w^{1118} ; *fic*^{30C}/CyO ; *Da*-Gal4,UAS^{Scer}-V5-Fic^{E247G}- $^{attP-B3}$/TM6B,hu

320 *BiP*^{G0102}/FM7c (BS#11815)

321 w^{1118};; p[gen3xFLAG-BiP^{WT}]$^{AttP-89E11}$

322 w^{1118};; p[gen3xFLAG-BiP^{T366A}]$^{AttP-89E11}$

323 w^{1118};; p[gen3xFLAG-BiP^{T518A}]$^{AttP-89E11}$

324 w^{1118} ; *fic*^{30C} ; p[gen3xFLAG-BiP^{WT}]$^{AttP-89E11}$

325 w^{1118} ; *fic*^{30C} ; p[gen3xFLAG-BiP^{T366A}]$^{AttP-89E11}$

326 w^{1118} ; *fic*^{30C} ; p[gen3xFLAG-BiP^{T518A}]$^{AttP-89E11}$

327 *BiP*^{G0102} ;; p[gen3xFLAG-BiP^{WT}]$^{AttP-89E11}$

328 *BiP*^{G0102} ;; p[gen3xFLAG-BiP^{T366A}]$^{AttP-89E11}$

329 *BiP*^{G0102} ; p[*GMR*-dsRNA^{white}]; p[gen3xFLAG-BiP^{WT}]^{89E11}

330 *BiP*^{G0102} ; p[*GMR*-dsRNA^{white}]; p[Attb_gen3xFLAG-BiP^{T366A}]^{89E11}

331 w^{1118} ; p[*tub-Atf4*$^{5'UTR}$-dsRed]/p[GMR-dsRNA^{white}]

332 w^{1118} ; *fic*^{30C},p[*tub-Atf4*$^{5'UTR}$-dsRed]/fic^{30C},p[*GMR*-dsRNA^{white}]

333 w^{1118} ; p[*GMR*-dsRNA^{white}] ; p[*Da*-Gal4]/p[UAS^{Scer}-Xbp1-GFP.hg]

334 w^{1118} ; *fic*^{30C},p[*GMR*-dsRNA^{white}] ; p[*Da*-Gal4]/p[UAS^{Scer}-Xbp1-GFP.hg]

335

bioRxiv preprint doi: https://doi.org/10.1101/348797; this version posted June 15, 2018. The copyright holder for this preprint (which was not certified by peer review) is the author/funder, who has granted bioRxiv a license to display the preprint in perpetuity. It is made available under aCC-BY 4.0 International license.

336 **Generation of genomic BiP transgenes**

337 BiP cDNA sequence were subcloned into a pAttB vector and a 3X-FLAG tag was
338 inserted after the N-terminal signal sequence. To create the T366A and T518A mutations,
339 gBlocks (IDT, Coralville, IA) for the mutant sequences were synthesized and subcloned into the
340 pAttB_genomic BiP vector via NEB HiFi Assembly Kit (NEB, Ipswich, MA). These constructs
341 were sequence-verified and injected into embryos (BestGene, Chino Hills, CA) for insertion at
342 the 89E11 landing site. Expression levels of FLAG-BiP transgenes were determined with
343 western blotting. In brief, fly heads were homogenized in lysis buffer (10% SDS, 6M urea, and
344 50mM Tris-HCl, pH 6.8+ 10% DTT), sonicated for 5 min, boiled for 2 min, and centrifuged for
345 10 min at 10,000 *g* to remove debris. 10µL were separated by SDS-PAGE and transferred to
346 nitrocellulose membranes. Blots were probed with anti-BiP (1:8000, gift from Dr. Don Ryoo,
347 NYU, NY), anti-FLAG (1:2000 M2- F3165, Millipore Sigma, St. Louis, MO) and anti-Actin
348 (1:4000, JLA-20, DSHB, Iowa City, IA) and detected using IRdye-labeled antibodies and an
349 Odyssey scanner (LI-COR Biosciences, Lincoln, NE).
350
351 **Generation of GMR_dsRNA^{white} transgenes**
352 To make the eye-targeted dsRNA constructs against the *white* gene, the dsRNA sequence
353 was obtained from a pAttb-UAS$^{S.cer}$-dsRNA^{white} vector (a gift from Dr. Dean Smith, UT
354 Southwestern Medical Center, TX) and the UAS$^{S.cer}$-Hsp40 promotor sequenced was replaced
355 with a 5X-*GMR* promotor sequence, synthesized as a gBlock (IDT) and cloned with NEB HiFi
356 Assembly Kit (NEB).
357

bioRxiv preprint doi: https://doi.org/10.1101/348797; this version posted June 15, 2018. The copyright holder for this preprint (which was not certified by peer review) is the author/funder, who has granted bioRxiv a license to display the preprint in perpetuity. It is made available under aCC-BY 4.0 International license.

Fly rearing conditions

All flies were reared on standard molasses fly food, under room temperature conditions. For light treatments, flies were collected within one to two days of enclosing, and placed in 5cm diameter vials containing normal food, with no more than 25 flies, and placed at either LD (lights ON 8am/lights OFF 8pm) or LL. ERGs, head dissections and behavior assays were performed between 1pm and 4pm. The same intensity white LED light source was used for both conditions and flies were kept the same distance away from the light source, which amounted to approximately 500 lux. LD and LL treatments were done at 25°C. For the UPR and Fic^{E247G} rough-eye interaction experiments, all flies were raised at 28°C.

Survival analysis of flies expressing genomic BiP construct

BiP^{G0102}/FM7c female virgin flies were crossed to males with either gen3xFLAG-BiP^{WT}, gen3xFLAG-BiP^{T366A} or gen3xFLAG-BiP^{T518A}. The number of surviving non-FM7c male flies were scored by presence or lack of the Bar eye marker. Percent of expected was calculated from the actual number or recovered flies of the relevant genotypes compared the expected Mendelian number [# observed flies/ #expected flies]. Crosses were repeated three times (n=3). Total number of flies scored was at least 100 for each BiP variant.

Survival analysis of flies expressing BiP variants in a *Da*-Gal4, UAS-Fic^{E247G} background

C-terminally V5-His6-tagged UAS-Fic^{E247G} (Casey et al., 2017) was expressed via the ubiquitous *Da*-Gal4 driver in *fic*^{30C}/CyO heterozygous flies. These flies were crossed to *w*$^{-}$*; fic*^{30C} (controls), *w*$^{-}$*; fic*^{30C}*;* gen3xFLAGBiP^{WT}, w-; *fic*^{30C}*;* gen3xFLAG^{T366A}, w-; *fic*^{30C}*;* gen3xFLAG-BiP^{T518A}, or *BiP*^{G0102}; *fic*^{30C}*;* gen3xFLAG^{T366A}. Offspring were scored and the number of adults

bioRxiv preprint doi: https://doi.org/10.1101/348797; this version posted June 15, 2018. The copyright holder for this preprint (which was not certified by peer review) is the author/funder, who has granted bioRxiv a license to display the preprint in perpetuity. It is made available under aCC-BY 4.0 International license.

homozygous for *fic*^{30C} with the *Da*-Gal4, UAS-Fic^{E247G} allele and were compared to the number of *fic*^{30C} heterozygous sibling controls. Percent of expected was calculated from the actual number or recovered flies of the relevant genotypes compared the expected Mendelian number [# observed flies/ #expected flies]. Crosses were repeated three times (n=3). Total number of flies scored was at least 100 for each BiP variant each repeat.

Electroretinograms

ERGs were recorded as previously described (Montell, 2012). Glass electrodes filled with 2M NaCl were placed in the fly thorax and surface of the corneal lens (recording). A computer-controlled LED light source (MC1500; Schott, Mainz, Germany) was pulsed for 1s at 4s intervals. The resulting ERG traces were collected by an electrometer (IE-210; Warner Instruments, Hamden, CT), digitized with a Digidata 1440A and MiniDigi 1B system (Molecular Devices, San Jose, CA), and recorded using Clampex 10.2 (Molecular Devices) and quantified with Clampfit software (Molecular Devices). Flies were assayed in batches of eight to ten, and resulting quantifications are pooled from three independent biological repeats.

Deep pseudopupil analysis

Flies were anesthetized on CO2 and aligned with one eye facing up. Using a stereoscopic dissection microscope, each fly was scored for presence or loss of the deep pseudopupil (Franceschini & Kirschfeld, 1971), and the percentage of flies with intact pseudopupils was calculated. For each genotype/treatment, over 50 flies were scored per replica and three biological replicas were performed (n=3).

bioRxiv preprint doi: https://doi.org/10.1101/348797; this version posted June 15, 2018. The copyright holder for this preprint (which was not certified by peer review) is the author/funder, who has granted bioRxiv a license to display the preprint in perpetuity. It is made available under aCC-BY 4.0 International license.

404 **Light-startle behavior assay**

405 Assay was adapted from a previously described method (Ni et al., 2017). After 72 hours
406 of LD or LL treatment, 16 flies per genotype were collected at the same time each morning and
407 placed into individual Drosophila Assay Monitoring (DAM) chambers (TriKinetics Inc,
408 Waltham, MA). The DAM monitors were placed into a dark incubator. Two hours later, a 500-
409 lux light was turned on by a timer for five minutes. Data was collected with DAMSystem3.0 and
410 DAMFileScan11.0 (TriKinetics Inc). The resulting data was exported to Microsoft Excel and
411 graphed in GraphPad Prism. Three replica experiments were averaged and plotted as Time (min)
412 vs Average activity per 2 min. bin (n=3). The change in response to light was calculated for each
413 light pulse as [*mean beam breaks for 10min. post-pulse*] – [*mean beam breaks for 10min. pre-*
414 *pulse*].

415

416 **Scanning electron microscopy**

417 SEMs of fly eyes were obtained as previously described (Wolff, 2011). Eyes were fixed
418 in 2% paraformaldehyde, 2% glutaraldehyde, 0.2% Tween 20, and 0.1 M cacodylate buffer, pH
419 7.4, for 2 hours. Samples were washed four times with increasing ethanol (25–100%) for 12
420 hours each followed by a series of hexamethyldisilazane washes (25–100% in ethanol) for one
421 hour each. Flies were air dried for 24 hours, mounted on SEM stubs, and the bodies were coated
422 in fast-drying silver paint. Flies were sputter coated with a gold/pallidum mixture for 60s and
423 imaged at 900X magnification, with extra high tension set at 3.0 kV on a scanning electron
424 microscope (Sigma SEM; Carl Zeiss, Germany). Ten flies per genotype were mounted and three
425 were imaged (n=3). Blinding of the samples' identity to the user acquiring the images was
426 performed.

bioRxiv preprint doi: https://doi.org/10.1101/348797; this version posted June 15, 2018. The copyright holder for this preprint (which was not certified by peer review) is the author/funder, who has granted bioRxiv a license to display the preprint in perpetuity. It is made available under aCC-BY 4.0 International license.

427

428 **Transmission electron microscopy**

429 TEMs of retina sections were performed as previously described (Jenny, 2011; Rahman
430 et al., 2012). Briefly, 550 nm sections were cut and stained with toluidine blue to confirm
431 orientation and section depth. Blocks were subsequently thin-sectioned at 70 nm with a diamond
432 knife (Diatome, Hatfield, PA) on a Leica Ultracut 6 ultramicrotome (Leica Microsystems,
433 Wetzlar, Germany) and collected onto formvar-coated, glow-discharged copper grids, post-
434 stained with 2% aqueous uranyl acetate and lead citrate. Images were acquired on a Tecnai G2
435 spirit transmission electron microscope (FEI) equipped with a LaB6 source using a voltage of
436 120 kV. Blinding of the samples to the technicians performing the processing and the user
437 acquiring the images was performed. Two fly heads per genotype/condition and at least three
438 thin sections per sample were examined (n=2). Samples were unmasked after the images were
439 processed.

440

441 **Immunohistochemistry for BiP and UPR reporters**

442 Fly heads were dissected in HL3 hemolymph-like solution, fixed for four hours in ice-
443 cold 4% para-formaldehyde in filtered PBS, washed overnight in 25% (wt/vol) sucrose in
444 phosphate buffer (pH 7.4), embedded in Optimal Cutting Temperature compound (EMS,
445 Hatfield, PA) frozen in dry ice and sectioned at 20-µm thickness on a cryostat microtome (CM
446 1950, Leica Microsystems, Wetzlar, Germany). Sections were probed overnight with primary
447 antibodies against Drosophila BiP (1:2000, Gift from Don Ryoo(Ryoo et al.), GFP (1:1000,
448 A10262, ThermoFisher Scientific, Waltham, MA) or RFP (1:1000, 600-401-379, Rockland,
449 Limerick, PA). Secondary antibodies were labeled with Alexa488-conjugated Goat anti-Chicken

bioRxiv preprint doi: https://doi.org/10.1101/348797; this version posted June 15, 2018. The copyright holder for this preprint (which was not certified by peer review) is the author/funder, who has granted bioRxiv a license to display the preprint in perpetuity. It is made available under aCC-BY 4.0 International license.

(Molecular Probes, P/N# A-11039), Alexa488-conjugated Goat anti-Guinea Pig (Molecular Probes, P/N# A-11073), or Alexa568-conjugated Goat anti-Rabbit (Molecular Probes, P/N# A-11011). Alexa 647-conjugated phallodin was also added to label Actin for identifying structures. Images were captured with an oil-immersion 63× NA-1.4 lens on an inverted confocal microscope (LSM710, Carl Zeiss). For each genotype and light rearing conditions, immunohistochemistry experiments were performed in two biological replicas with new sets of flies, using identical acquisition settings. Blinding of the samples to the user acquiring the images was performed when appropriate.

Quantification of fluorescence staining

Fluorescence images were quantified using ImageJ (NIH) adapting previous methods (Nandi et al., 2017). For each antibody, a threshold was determined, removing the lowest 10% of signal in LD control samples (to reduce variation from low level background signals). This same threshold was applied, and a mask was created for every image in a batch of staining. Within a 1-μm optical slice, the retina and lamina regions were selected manually using an Actin stain and assigned as Regions of Interest. The integrated pixel intensity per unit area was measured within this selected area, redirecting to the threshold mask. In each fly, four sequential optical slices were quantified and averaged. For each genotype and treatment, four flies were quantified from two independent biological replicas for a total of eight flies. Data was normalized to the wild-type LD control for each replica. Outliers of greater than three standard deviations were omitted from the analysis.

bioRxiv preprint doi: https://doi.org/10.1101/348797; this version posted June 15, 2018. The copyright holder for this preprint (which was not certified by peer review) is the author/funder, who has granted bioRxiv a license to display the preprint in perpetuity. It is made available under aCC-BY 4.0 International license.

Yeast plasmids and strains

Yeast genetic techniques were performed by standard procedures described previously. (Sherman et al., 1981). All strains were cultured in either rich (YPD: 1% yeast extract, 2% peptone, and 2% glucose) or complete synthetic minimal (CSM) media lacking appropriate amino acids with 2% glucose. Yeast were grown to log phase, serially diluted, and spotted onto agar plates to assay fitness and temperature sensitivity as previously described (Tran et al., 2007).

DNA fragments of KAR2 was generated by PCR amplification of the endogenous KAR2 gene using the primers 5'-GCATCCGCGGATACTCTCGTACCCTGCCGC-3' and 5'-ATGCGAGCTCCGTATATACTCAGTATAATC-3'. Plasmid pKAR2:LEU2 and pKAR2:URA3 were generated by subcloning genomic DNA fragments containing promoter and coding sequence of *KAR2* into the *Sac*I and *Sac*II sites of pRS315 and pRS316, respectively. pKAR2T386A:LEU2 was generated by site directed mutagenesis of pKAR2:LEU2 using the primers 5'-GGTTGGTGGTTCTGCTAGAATTCCAAAGGTCCAACAATTGTTAGAATCATACTTTGATGG-3' and 5'-ACCTTTGGAATTCTAGCAGAACCACCAACCAAAACGATATCATCAACATCCTTCTTTTCC-3'. pKAR2T538A:LEU2 was generated by site directed mutagenesis of pKAR2:LEU2 using the primers 5'-AGATAAGGGAGCTGGTAAATCCGAATCTATCACCATCACTAACG-3' and 5'-GGATTTACCAGCTCCCTTATCTGTGGCAGACACCTTCAGAATACC-3'.

ACY008 yeast (mat A kar2::KAN his3Δ0 leu2Δ0 LYS met15Δ0 ura3Δ0 pKAR2:URA) were obtained by sporulation and dissection of KAR2 heterozygous null yeast (Mata/mat@ KAR2::KAN/KAR2 his3Δ0/his3Δ0 leu2Δ0/leu2Δ0 LYS/lys MET/met15Δ0 ura3Δ0/ura3Δ0) (GE) transformed with pKAR2:URA. Standard plasmid shuffle techniques with 5-FOA(Zymo)

bioRxiv preprint doi: https://doi.org/10.1101/348797; this version posted June 15, 2018. The copyright holder for this preprint (which was not certified by peer review) is the author/funder, who has granted bioRxiv a license to display the preprint in perpetuity. It is made available under aCC-BY 4.0 International license.

were utilized to obtain ACY016 (mat A kar2::KAN his3Δ0 leu2Δ0 LYS met15Δ0 ura3Δ0 pKAR2:LEU2) ACY017(mat A kar2::KAN his3Δ0 leu2Δ0 LYS met15Δ0 ura3Δ0 pKAR2T386A:LEU2), and ACY020(mat A kar2::KAN his3Δ0 leu2Δ0 LYS met15Δ0 ura3Δ0 pKAR2T538A:LEU2)

Statistics

Statistics were performed using GraphPad Prism 7. Normality of data distribution was determined using D'Agostino's & Pearson's normality test. For the genetic analysis in Figure 1 and the ERG measurements in Supplemental Figures 2,3,5, and 6, significance was determined using one-way ANOVA, followed by Tukey's multiple comparisons tests. Statistical significance for non-parametric data, including the ERGs with light treatment quantifications in Figure 2, was determined by Kruskal-Wallis tests followed by multiple comparisons testing with Dunn's correction. For the image quantification data in Figure 4, significance was determined by two-way ANOVA followed by multiple comparisons with Benjamini-Krieger-Yekutieli's False Discovery Rate correction. All tests were two-sided with no experimental matching. RStudio (version 1.1.442, 2018, RStudio, Inc.) was used for Fisher's Exact Tests for the eye interaction screen, with Bonferroni's multiple comparison method to determine significance. Standard R functions were used, no custom scripts were developed. Tests were two-sided. When possible, blinding of sample identities was performed for image acquisition and fluorescence intensity quantification. Sample sizes for ERG assays, EM experiments, fluorescence quantifications and fly genetic analysis were determined based from previous experience (Nandi et al., 2017; Rahman et al., 2012; Stenesen et al., 2015).

bioRxiv preprint doi: https://doi.org/10.1101/348797; this version posted June 15, 2018. The copyright holder for this preprint (which was not certified by peer review) is the author/funder, who has granted bioRxiv a license to display the preprint in perpetuity. It is made available under aCC-BY 4.0 International license.

Competing Interests:

The authors declare no competing interests.

bioRxiv preprint doi: https://doi.org/10.1101/348797; this version posted June 15, 2018. The copyright holder for this preprint (which was not certified by peer review) is the author/funder, who has granted bioRxiv a license to display the preprint in perpetuity. It is made available under aCC-BY 4.0 International license.

References:

Akbar, M. A., Ray, S., & Krämer, H. (2009). The SM protein Car/Vps33A regulates SNARE-mediated trafficking to lysosomes and lysosome-related organelles. *Mol Biol Cell, 20*(6), 1705-1714. doi:10.1091/mbc.E08-03-0282

Amin-Wetzel, N., Saunders, R. A., Kamphuis, M. J., Rato, C., Preissler, S., Harding, H. P., & Ron, D. (2017). A J-Protein Co-chaperone Recruits BiP to Monomerize IRE1 and Repress the Unfolded Protein Response. *Cell, 171*(7), 1625-1637 e1613. doi:10.1016/j.cell.2017.10.040

Bertolotti, A., Zhang, Y., Hendershot, L. M., Harding, H. P., & Ron, D. (2000). Dynamic interaction of BiP and ER stress transducers in the unfolded-protein response. *Nat Cell Biol, 2*(6), 326-332. doi:10.1038/35014014

Borycz, J., Borycz, J. A., Loubani, M., & Meinertzhagen, I. A. (2002). tan and ebony genes regulate a novel pathway for transmitter metabolism at fly photoreceptor terminals. *J Neurosci, 22*(24), 10549-10557.

Brown, M. S., Segal, A., & Stadtman, E. R. (1971). Modulation of glutamine synthetase adenylylation and deadenylylation is mediated by metabolic transformation of the P II -regulatory protein. *Proc Natl Acad Sci U S A, 68*(12), 2949-2953.

Carrara, M., Prischi, F., Nowak, P. R., Kopp, M. C., & Ali, M. M. (2015). Noncanonical binding of BiP ATPase domain to Ire1 and Perk is dissociated by unfolded protein CH1 to initiate ER stress signaling. *Elife, 4*. doi:10.7554/eLife.03522

Casey, A. K., Moehlman, A. T., Zhang, J., Servage, K. A., Krämer, H., & Orth, K. (2017). Fic-mediated deAMPylation is not dependent on homodimerization and rescues toxic AMPylation in flies. *J Biol Chem, 292*(51), 21193-21204. doi:10.1074/jbc.M117.799296

Casey, A. K., & Orth, K. (2018). Enzymes Involved in AMPylation and deAMPylation. *Chem Rev, 118*(3), 1199-1215. doi:10.1021/acs.chemrev.7b00145

Colley, N. J., Cassill, J. A., Baker, E. K., & Zuker, C. S. (1995). Defective intracellular transport is the molecular basis of rhodopsin-dependent dominant retinal degeneration. *Proc Natl Acad Sci U S A, 92*(7).

Damulewicz, M., Mazzotta, G. M., Sartori, E., Rosato, E., Costa, R., & Pyza, E. M. (2017). Cryptochrome Is a Regulator of Synaptic Plasticity in the Visual System of Drosophila melanogaster. *Front Mol Neurosci, 10*, 165. doi:10.3389/fnmol.2017.00165

Dietzl, G., Chen, D., Schnorrer, F., Su, K. C., Barinova, Y., Fellner, M., . . . Dickson, B. J. (2007). A genome-wide transgenic RNAi library for conditional gene inactivation in Drosophila. *Nature, 448*(7150), 151-156. doi:10.1038/nature05954

Dolph, P. J., Ranganathan, R., Colley, N. J., Hardy, R. W., Socolich, M., & Zuker, C. S. (1993). Arrestin function in inactivation of G protein-coupled receptor rhodopsin in vivo. *Science, 260*(5116), 1910-1916.

Franceschini, N., & Kirschfeld, K. (1971). [Pseudopupil phenomena in the compound eye of drosophila]. *Kybernetik, 9*(5), 159-182.

Gardner, B. M., Pincus, D., Gotthardt, K., Gallagher, C. M., & Walter, P. (2013). Endoplasmic reticulum stress sensing in the unfolded protein response. *Cold Spring Harb Perspect Biol, 5*(3), a013169. doi:10.1101/cshperspect.a013169

Gaut, J. R., & Hendershot, L. M. (1993). Mutations within the nucleotide binding site of immunoglobulin-binding protein inhibit ATPase activity and interfere with release of immunoglobulin heavy chain. *J Biol Chem, 268*(10), 7248-7255.

bioRxiv preprint doi: https://doi.org/10.1101/348797; this version posted June 15, 2018. The copyright holder for this preprint (which was not certified by peer review) is the author/funder, who has granted bioRxiv a license to display the preprint in perpetuity. It is made available under aCC-BY 4.0 International license.

565 Ham, H., Woolery, A. R., Tracy, C., Stenesen, D., Krämer, H., & Orth, K. (2014). Unfolded
566 protein response-regulated Drosophila Fic (dFic) protein reversibly AMPylates BiP
567 chaperone during endoplasmic reticulum homeostasis. *J Biol Chem, 289*(52), 36059-
568 36069. doi:10.1074/jbc.M114.612515
569 Harms, A., Stanger, F. V., & Dehio, C. (2016). Biological Diversity and Molecular Plasticity of
570 FIC Domain Proteins. *Annu Rev Microbiol, 70*, 341-360. doi:10.1146/annurev-micro-
571 102215-095245
572 Hendershot, L. M., Ting, J., & Lee, A. S. (1988). Identity of the immunoglobulin heavy-chain-
573 binding protein with the 78,000-dalton glucose-regulated protein and the role of
574 posttranslational modifications in its binding function. *Mol Cell Biol, 8*(10), 4250-4256.
575 Jenny, A. (2011). Preparation of adult Drosophila eyes for thin sectioning and microscopic
576 analysis. *J Vis Exp*(54). doi:10.3791/2959
577 Johnson, K., Grawe, F., Grzeschik, N., & Knust, E. (2002). Drosophila crumbs is required to
578 inhibit light-induced photoreceptor degeneration. *Curr Biol, 12*(19), 1675-1680.
579 Kang, K., Ryoo, H. D., Park, J. E., Yoon, J. H., & Kang, M. J. (2015). A Drosophila Reporter for
580 the Translational Activation of ATF4 Marks Stressed Cells during Development. *PLoS*
581 *One, 10*(5), e0126795. doi:10.1371/journal.pone.0126795
582 Kingdon, H. S., Shapiro, B. M., & Stadtman, E. R. (1967). Regulation of glutamine synthetase.
583 8. ATP: glutamine synthetase adenylyltransferase, an enzyme that catalyzes alterations in
584 the regulatory properties of glutamine synthetase. *Proc Natl Acad Sci U S A, 58*(4), 1703-
585 1710.
586 Kiselev, A., Socolich, M., Vinos, J., Hardy, R. W., Zuker, C. S., & Ranganathan, R. (2000). A
587 molecular pathway for light-dependent photoreceptor apoptosis in Drosophila. *Neuron,*
588 *28*(1), 139-152.
589 Kozutsumi, Y., Segal, M., Normington, K., Gething, M. J., & Sambrook, J. (1988). The presence
590 of malfolded proteins in the endoplasmic reticulum signals the induction of glucose-
591 regulated proteins. *Nature, 332*(6163), 462-464. doi:10.1038/332462a0
592 Lee, S. J., & Montell, C. (2004). Suppression of constant-light-induced blindness but not retinal
593 degeneration by inhibition of the rhodopsin degradation pathway. *Curr Biol, 14*(23),
594 2076-2085. doi:10.1016/j.cub.2004.11.054
595 Lee, S. J., Xu, H., Kang, L. W., Amzel, L. M., & Montell, C. (2003). Light adaptation through
596 phosphoinositide-regulated translocation of Drosophila visual arrestin. *Neuron, 39*(1),
597 121-132.
598 Leonard, D. S., Bowman, V. D., Ready, D. F., & Pak, W. L. (1992). Degeneration of
599 photoreceptors in rhodopsin mutants of Drosophila. *J Neurobiol, 23*(6), 605-626.
600 doi:10.1002/neu.480230602
601 Ma, Y., & Hendershot, L. M. (2003). Delineation of a negative feedback regulatory loop that
602 controls protein translation during endoplasmic reticulum stress. *J Biol Chem, 278*(37),
603 34864-34873. doi:10.1074/jbc.M301107200
604 Meunier, L., Usherwood, Y. K., Chung, K. T., & Hendershot, L. M. (2002). A subset of
605 chaperones and folding enzymes form multiprotein complexes in endoplasmic reticulum
606 to bind nascent proteins. *Mol Biol Cell, 13*(12), 4456-4469. doi:10.1091/mbc.E02-05-
607 0311
608 Montell, C. (2012). Drosophila visual transduction. *Trends Neurosci, 35*(6), 356-363.
609 doi:10.1016/j.tins.2012.03.004

bioRxiv preprint doi: https://doi.org/10.1101/348797; this version posted June 15, 2018. The copyright holder for this preprint (which was not certified by peer review) is the author/funder, who has granted bioRxiv a license to display the preprint in perpetuity. It is made available under aCC-BY 4.0 International license.

Nandi, N., Tyra, L. K., Stenesen, D., & Krämer, H. (2017). Stress-induced Cdk5 activity enhances cytoprotective basal autophagy in Drosophila melanogaster by phosphorylating acinus at serine(437). *Elife, 6*. doi:10.7554/eLife.30760

Ni, J. D., Baik, L. S., Holmes, T. C., & Montell, C. (2017). A rhodopsin in the brain functions in circadian photoentrainment in Drosophila. *Nature, 545*(7654), 340-344. doi:10.1038/nature22325

Preissler, S., Rato, C., Chen, R., Antrobus, R., Ding, S., Fearnley, I. M., & Ron, D. (2015). AMPylation matches BiP activity to client protein load in the endoplasmic reticulum. *Elife, 4*, e12621. doi:10.7554/eLife.12621

Preissler, S., Rato, C., Perera, L., Saudek, V., & Ron, D. (2017). FICD acts bifunctionally to AMPylate and de-AMPylate the endoplasmic reticulum chaperone BiP. *Nat Struct Mol Biol, 24*(1), 23-29. doi:10.1038/nsmb.3337

Preissler, S., Rohland, L., Yan, Y., Chen, R., Read, R. J., & Ron, D. (2017). AMPylation targets the rate-limiting step of BiP's ATPase cycle for its functional inactivation. *Elife, 6*. doi:10.7554/eLife.29428

Rahman, M., Ham, H., Liu, X., Sugiura, Y., Orth, K., & Kramer, H. (2012). Visual neurotransmission in Drosophila requires expression of Fic in glial capitate projections. *Nat Neurosci, 15*(6), 871-875. doi:10.1038/nn.3102

Rosenbaum, E. E., Hardie, R. C., & Colley, N. J. (2006). Calnexin is essential for rhodopsin maturation, Ca2+ regulation, and photoreceptor cell survival. *Neuron, 49*(2), 229-241. doi:10.1016/j.neuron.2005.12.011

Ryoo, H. D., Domingos, P. M., Kang, M. J., & Steller, H. (2007). Unfolded protein response in a Drosophila model for retinal degeneration. *EMBO J, 26*(1), 242-252. doi:10.1038/sj.emboj.7601477

Scott, K., Becker, A., Sun, Y., Hardy, R., & Zuker, C. (1995). Gq alpha protein function in vivo: genetic dissection of its role in photoreceptor cell physiology. *Neuron, 15*(4), 919-927.

Shen, J., Snapp, E. L., Lippincott-Schwartz, J., & Prywes, R. (2005). Stable binding of ATF6 to BiP in the endoplasmic reticulum stress response. *Mol Cell Biol, 25*(3), 921-932. doi:10.1128/MCB.25.3.921-932.2005

Sherman, F., Fink, G. R., Hicks, J. B., & Laboratory, C. S. H. (1981). *Methods in yeast genetics*: Cold Spring Harbor Laboratory.

Smith, D. P., Ranganathan, R., Hardy, R. W., Marx, J., Tsuchida, T., & Zuker, C. S. (1991). Photoreceptor deactivation and retinal degeneration mediated by a photoreceptor-specific protein kinase C. *Science, 254*(5037), 1478-1484.

Sone, M., Zeng, X., Larese, J., & Ryoo, H. D. (2013). A modified UPR stress sensing system reveals a novel tissue distribution of IRE1/XBP1 activity during normal Drosophila development. *Cell Stress Chaperones, 18*(3), 307-319. doi:10.1007/s12192-012-0383-x

Soukup, S. F., Pocha, S. M., Yuan, M., & Knust, E. (2013). DLin-7 is required in postsynaptic lamina neurons to prevent light-induced photoreceptor degeneration in Drosophila. *Curr Biol, 23*(14), 1349-1354. doi:10.1016/j.cub.2013.05.060

Stenesen, D., Moehlman, A. T., & Krämer, H. (2015). The carcinine transporter CarT is required in Drosophila photoreceptor neurons to sustain histamine recycling. *Elife, 4*, e10972. doi:10.7554/eLife.10972

Sugie, A., Hakeda-Suzuki, S., Suzuki, E., Silies, M., Shimozono, M., Mohl, C., . . . Tavosanis, G. (2015). Molecular Remodeling of the Presynaptic Active Zone of Drosophila

bioRxiv preprint doi: https://doi.org/10.1101/348797; this version posted June 15, 2018. The copyright holder for this preprint (which was not certified by peer review) is the author/funder, who has granted bioRxiv a license to display the preprint in perpetuity. It is made available under aCC-BY 4.0 International license.

Photoreceptors via Activity-Dependent Feedback. *Neuron, 86*(3), 711-725. doi:10.1016/j.neuron.2015.03.046

Tran, E. J., Zhou, Y., Corbett, A. H., & Wente, S. R. (2007). The DEAD-box protein Dbp5 controls mRNA export by triggering specific RNA:protein remodeling events. *Mol Cell, 28*(5), 850-859. doi:10.1016/j.molcel.2007.09.019

Truttmann, M. C., Cruz, V. E., Guo, X., Engert, C., Schwartz, T. U., & Ploegh, H. L. (2016). The Caenorhabditis elegans Protein FIC-1 Is an AMPylase That Covalently Modifies Heat-Shock 70 Family Proteins, Translation Elongation Factors and Histones. *PLoS Genet, 12*(5), e1006023. doi:10.1371/journal.pgen.1006023

Truttmann, M. C., Zheng, X., Hanke, L., Damon, J. R., Grootveld, M., Krakowiak, J., . . . Ploegh, H. L. (2017). Unrestrained AMPylation targets cytosolic chaperones and activates the heat shock response. *Proc Natl Acad Sci U S A, 114*(2), E152-E160. doi:10.1073/pnas.1619234114

Venken, K. J., He, Y., Hoskins, R. A., & Bellen, H. J. (2006). P[acman]: a BAC transgenic platform for targeted insertion of large DNA fragments in D. melanogaster. *Science, 314*(5806), 1747-1751. doi:10.1126/science.1134426

Wieteska, L., Shahidi, S., & Zhuravleva, A. (2017). Allosteric fine-tuning of the conformational equilibrium poises the chaperone BiP for post-translational regulation. *Elife, 6*. doi:10.7554/eLife.29430

Wolff, T. (2011). Preparation of Drosophila eye specimens for scanning electron microscopy. *Cold Spring Harb Protoc, 2011*(11), 1383-1385. doi:10.1101/pdb.prot066506

Woolery, A. R., Yu, X., LaBaer, J., & Orth, K. (2014). AMPylation of Rho GTPases subverts multiple host signaling processes. *J Biol Chem, 289*(47), 32977-32988. doi:10.1074/jbc.M114.601310

Acknowledgments:

We thank Drs. Eric Olson and Joe Takahashi and the members of the Kramer and Orth labs for discussion and technical assistance. We thank the Bloomington Stock Center (NIH P40OD018537) and the Vienna Drosophila Resource Center (VDRC, www.vdrc.at) for flies and the Molecular and Cellular Imaging Facility at the University of Texas Southwestern Medical center for help with electron microscopy (NIH S10 OD020103-01).

Funding: K.O. is a Burroughs Welcome Investigator in Pathogenesis of Infectious Disease, a Beckman Young Investigator, and a W. W. Caruth, Jr., Biomedical Scholar and has an Earl A. Forsythe Chair in Biomedical Science.

bioRxiv preprint doi: https://doi.org/10.1101/348797; this version posted June 15, 2018. The copyright holder for this preprint (which was not certified by peer review) is the author/funder, who has granted bioRxiv a license to display the preprint in perpetuity. It is made available under aCC-BY 4.0 International license.

693

694 **Author contributions:**

695 A.T.M, A.C. K.O and H.K. conceived, designed, and analyzed experiments and wrote the
696 manuscript. All experiments except yeast experiments were performed by A.T.M. A.C. and K.S.
697 performed mass spec experiments.

698

699 **Data and materials availability:** Fly stocks are available upon request. All data are contained
700 in the source files.

701

702 **Correspondence to:** Helmut.Kramer@UTSouthwestern.edu and
703 Kim.Orth@utsouthwestern.edu.

704

bioRxiv preprint doi: https://doi.org/10.1101/348797; this version posted June 15, 2018. The copyright holder for this preprint (which was not certified by peer review) is the author/funder, who has granted bioRxiv a license to display the preprint in perpetuity. It is made available under aCC-BY 4.0 International license.

Figures

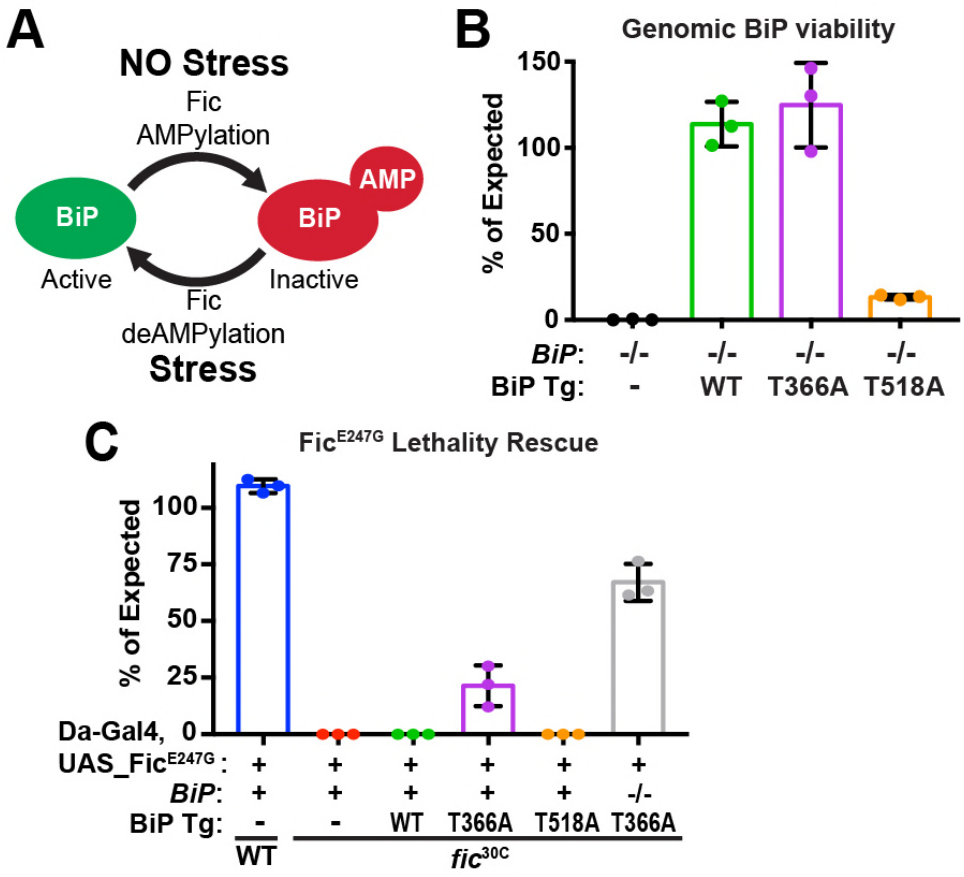

Figure 1. BiP is a target of Fic AMPylation and deAMPylation *in vivo*. (A) BiP AMPylation during times of low ER stress reserves a portion of the chaperone to allow for a rapid, deAMPylation-driven, response to high ER stress (Casey et al., 2017; Preissler, Rato, et al., 2017). **(B)** Bar graphs show the percentage of null mutant BiP^{G0102}/y males rescued by the indicated genomic BiP^{WT}, BiP^{T366A} or BiP^{T518A} genomic transgene (Tg) relative to sibling controls. N=3 biological replicas. At least 50 flies scored for each replica. Bar graphs show means +/- Standard Deviation (SD). **(C)** Bar graphs show the percentage of viable flies of the indicated wild type or fic^{30C} genotypes expressing the overactive Fic^{E247G} under the ubiquitous Da-Gal4 driver relative to sibling controls. Among the indicated genomic BiP transgenes, only BiP^{T366A} provides partial rescue of lethality in the $BiP^{+/+}$ background and near complete rescue in a BiP^{G0102} null background. N=3 biological replicas. At least 100 total flies scored for each replica. Bar graphs show means +/- SD.

bioRxiv preprint doi: https://doi.org/10.1101/348797; this version posted June 15, 2018. The copyright holder for this preprint (which was not certified by peer review) is the author/funder, who has granted bioRxiv a license to display the preprint in perpetuity. It is made available under aCC-BY 4.0 International license.

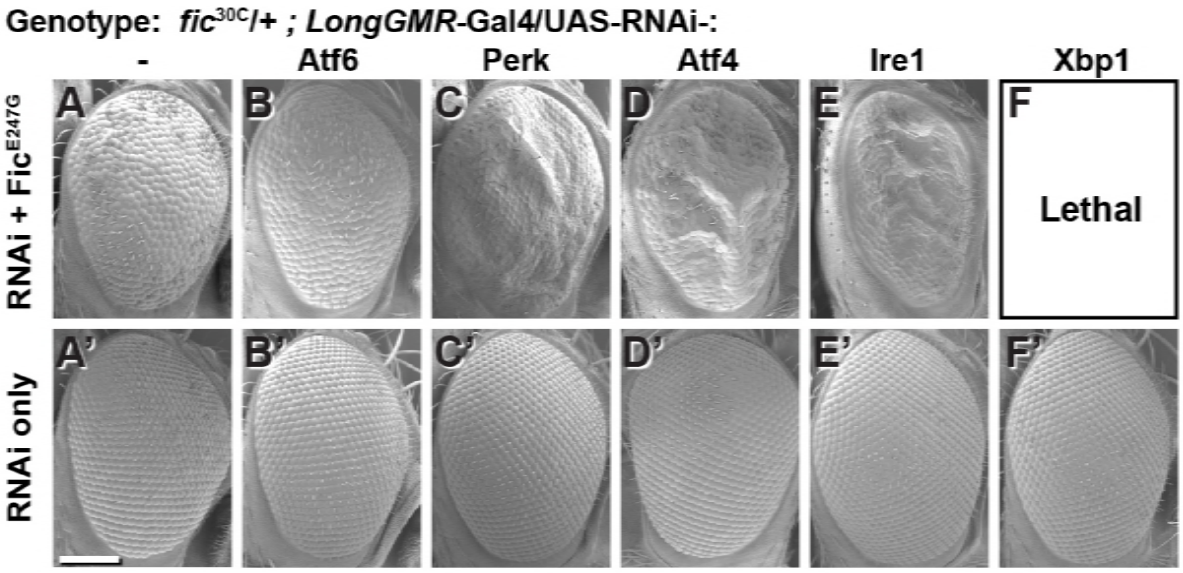

719

720 **Figure 2. Genetic interactions between Fic and UPR genes.** Representative SEM images of
721 heterozygote mutant *fic*$^{30C/+}$ eyes expressing the indicated UAS-RNAi transgenes with (A-F) or
722 without (A'-F') UAS-Fic^{E247G} under *longGMR*-Gal4 control. See Supplemental Table 1 for
723 quantification. Scale bar: 100µM.

bioRxiv preprint doi: https://doi.org/10.1101/348797; this version posted June 15, 2018. The copyright holder for this preprint (which was not certified by peer review) is the author/funder, who has granted bioRxiv a license to display the preprint in perpetuity. It is made available under aCC-BY 4.0 International license.

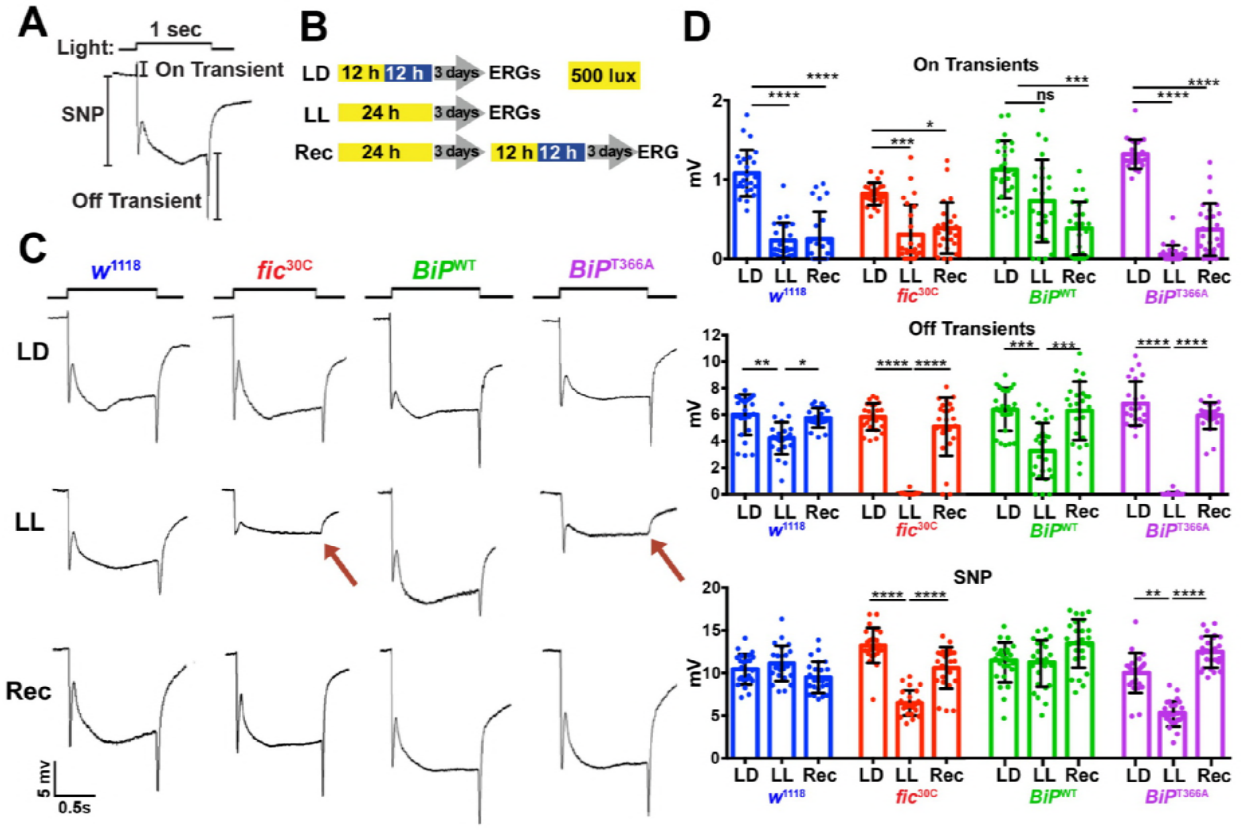

Figure 3. Fic-mediated AMPylation of BiP is required for photoreceptor maintenance. (A) A representative ERG trace in response to a 1-sec light pulse displaying the sustained negative potential (SNP), representing the depolarization within photoreceptor neurons, and the ON & OFF transients, reflecting post-synaptic activity of lamina neurons. **(B)** Representation of the different light treatments of flies before ERG recordings: 3 days of 12hr light (500 lux) and 12hr dark (LD), 3 days of continuous light (LL) or 3 days of continuous light followed by 3 days of LD (Rec). 1-sec light pulses were performed at 4 sec intervals. **(C)** Representative traces from w^{1118}, fic^{30C}, BiP^{WT} and BiP^{T366A} flies. Under LL, fic^{30C} and BiP^{T366A} mutants lose ON and OFF transients (red arrows) and have reduced SNPs. The changes are reversed after 3-days of recovery (Rec). **(D)** Quantification of key components of ERGs shown in panel C. Bar graphs show means +/- SD. ****, $p < 0.0001$; ***, $p < 0.001$; **, $p < 0.01$; *, $p < 0.05$; n= 24 flies for each genotype/condition, pooled from three independent biological replicas.

bioRxiv preprint doi: https://doi.org/10.1101/348797; this version posted June 15, 2018. The copyright holder for this preprint (which was not certified by peer review) is the author/funder, who has granted bioRxiv a license to display the preprint in perpetuity. It is made available under aCC-BY 4.0 International license.

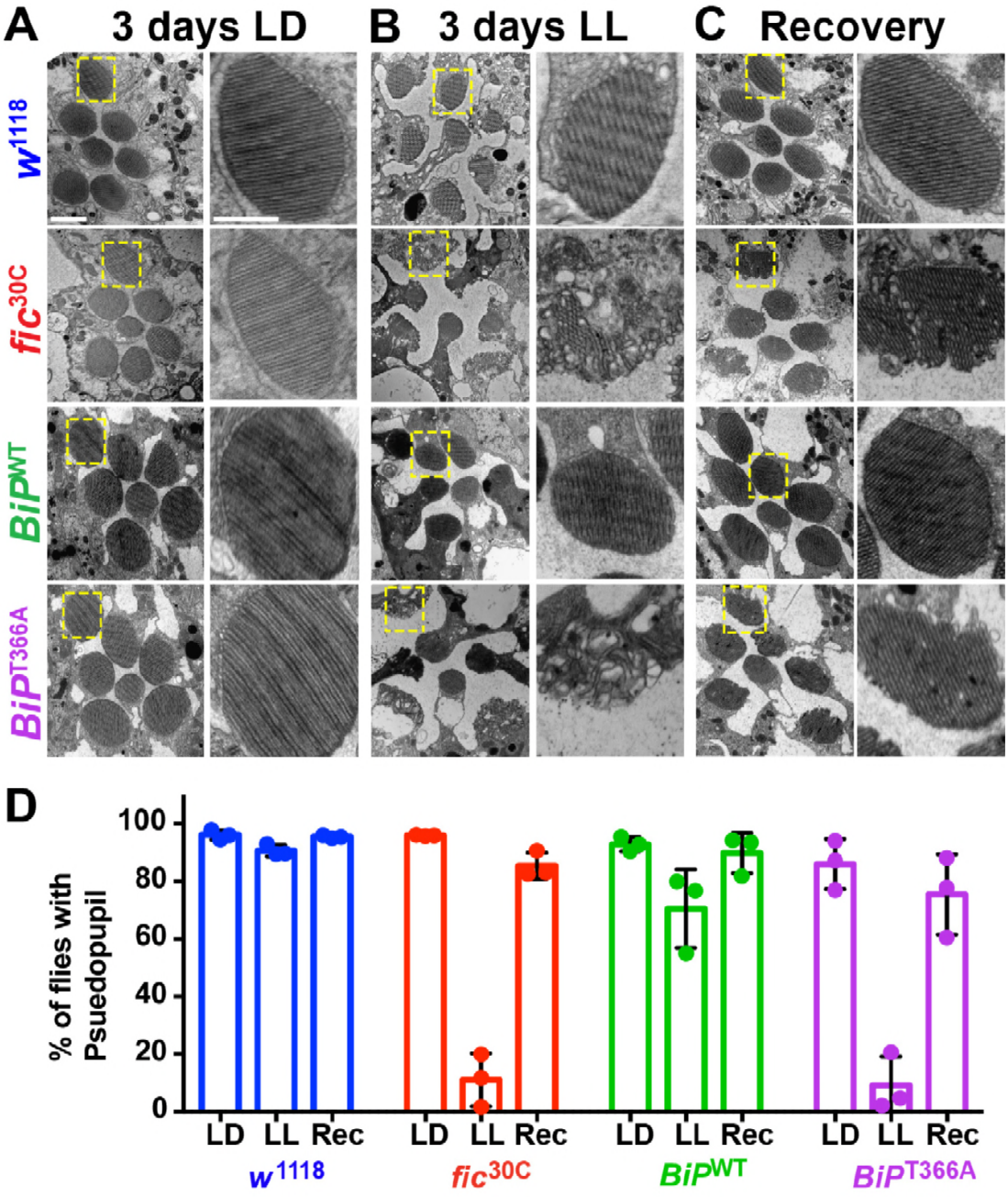

Figure 4. AMPylation of BiP is required for maintaining structural plasticity in the retina. **(A-C)** Representative TEM images of retina thin sections from the indicated genotypes with either standard LD **(A)**, the stress-inducing LL **(B)** or recovery treatment **(C)**. Scale bars: 1 µM. Yellow boxes indicate rhabdomeres shown in high magnification images. High magnification scale bars: 0.5 µM. **(D)** Percentages of flies with intact deep pseudopupil following LD, LL and Rec. N=3 independent biological replicas with approximately 50 flies scored per genotype per replica. Bar graphs show means +/- SD.

bioRxiv preprint doi: https://doi.org/10.1101/348797; this version posted June 15, 2018. The copyright holder for this preprint (which was not certified by peer review) is the author/funder, who has granted bioRxiv a license to display the preprint in perpetuity. It is made available under aCC-BY 4.0 International license.

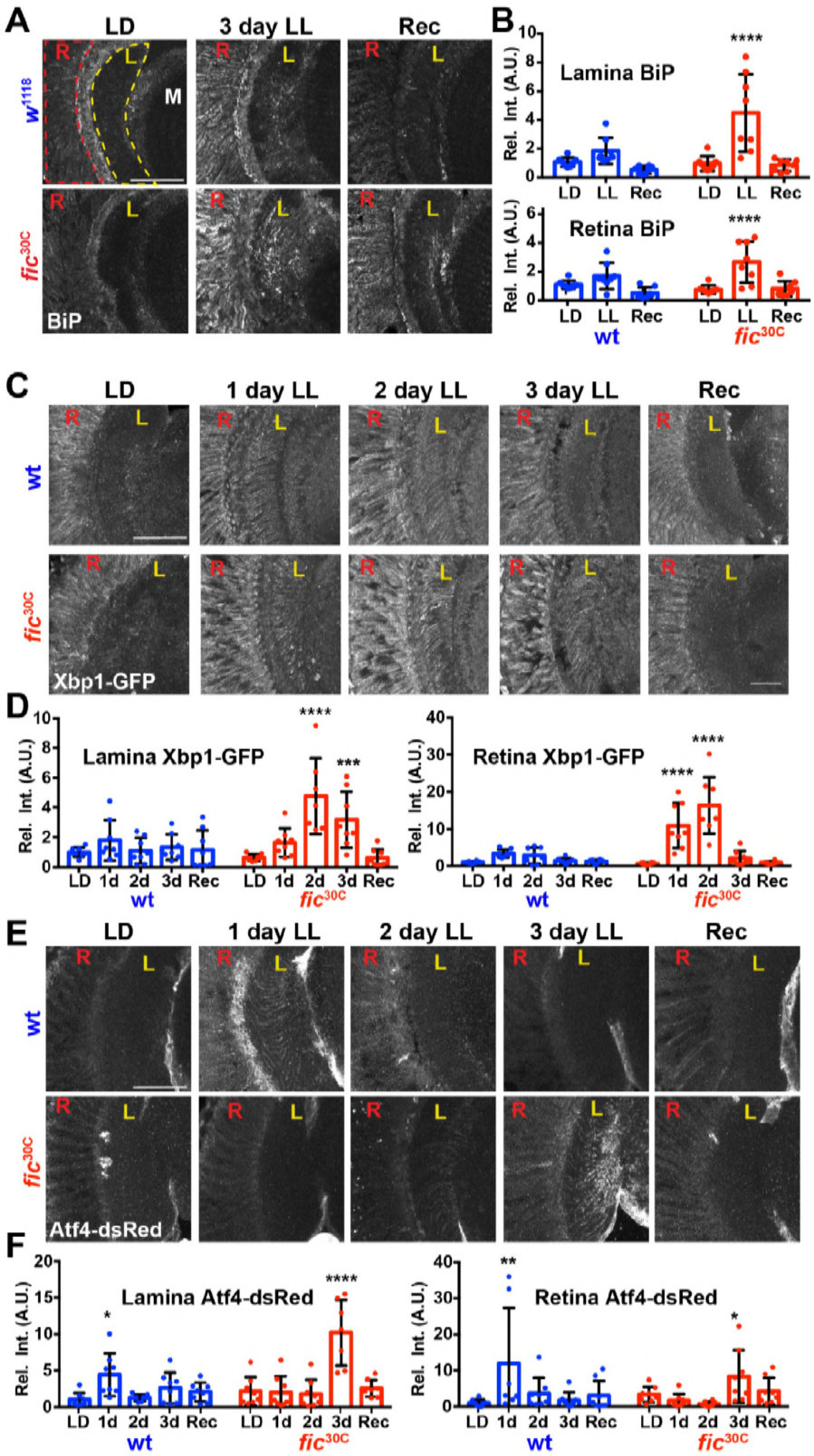

Figure 5. BiP AMPylation regulates ER homeostasis during prolonged light stimulation.

(A) Representative images of BiP immunohistochemistry in sections of w^{1118} and fic^{30C} flies

bioRxiv preprint doi: https://doi.org/10.1101/348797; this version posted June 15, 2018. The copyright holder for this preprint (which was not certified by peer review) is the author/funder, who has granted bioRxiv a license to display the preprint in perpetuity. It is made available under aCC-BY 4.0 International license.

following 3 days LD, LL or Recovery treatments. **(B)** Quantification of BiP fluorescence intensity, normalized to wild-type LD controls, in the lamina neuropil and retina from 2 independent experiments. **(C)** Representative images of a Xbp1-GFP splicing reporter in either a Fic wild-type or the null *fic*^{30C} background following LD, 1-day LL, 2-day LL, 3-day LL, and Recovery conditions. **(D)** Quantification of GFP fluorescence intensity, normalized to wild-type LD controls, in the lamina neuropil and retina from 2 independent experiments. **(E)** Representative images of an *Atf4*-dsRed reporter in either a wild-type or *fic*^{30C} background following LD, 1-day LL, 2-day LL, 3-day LL, and Recovery conditions. **(F)** Quantification of *Atf4*-dsRed intensity, normalized to wild-type LD controls, in the lamina neuropil and retina from 2 independent experiments. For all experiments, n= 8 flies per genotype/condition, with exceptions of outliers falling 3 standard deviations outside the mean. Bar graphs show means +/- SD. For all experiments, significance is indicated for treatment compared to the LD condition for the corresponding genotype. ****, $p < 0.0001$; ***, $p < 0.001$; **, $p < 0.01$; *, $p < 0.05$. All scale bars: 50 μM.

bioRxiv preprint doi: https://doi.org/10.1101/348797; this version posted June 15, 2018. The copyright holder for this preprint (which was not certified by peer review) is the author/funder, who has granted bioRxiv a license to display the preprint in perpetuity. It is made available under aCC-BY 4.0 International license.

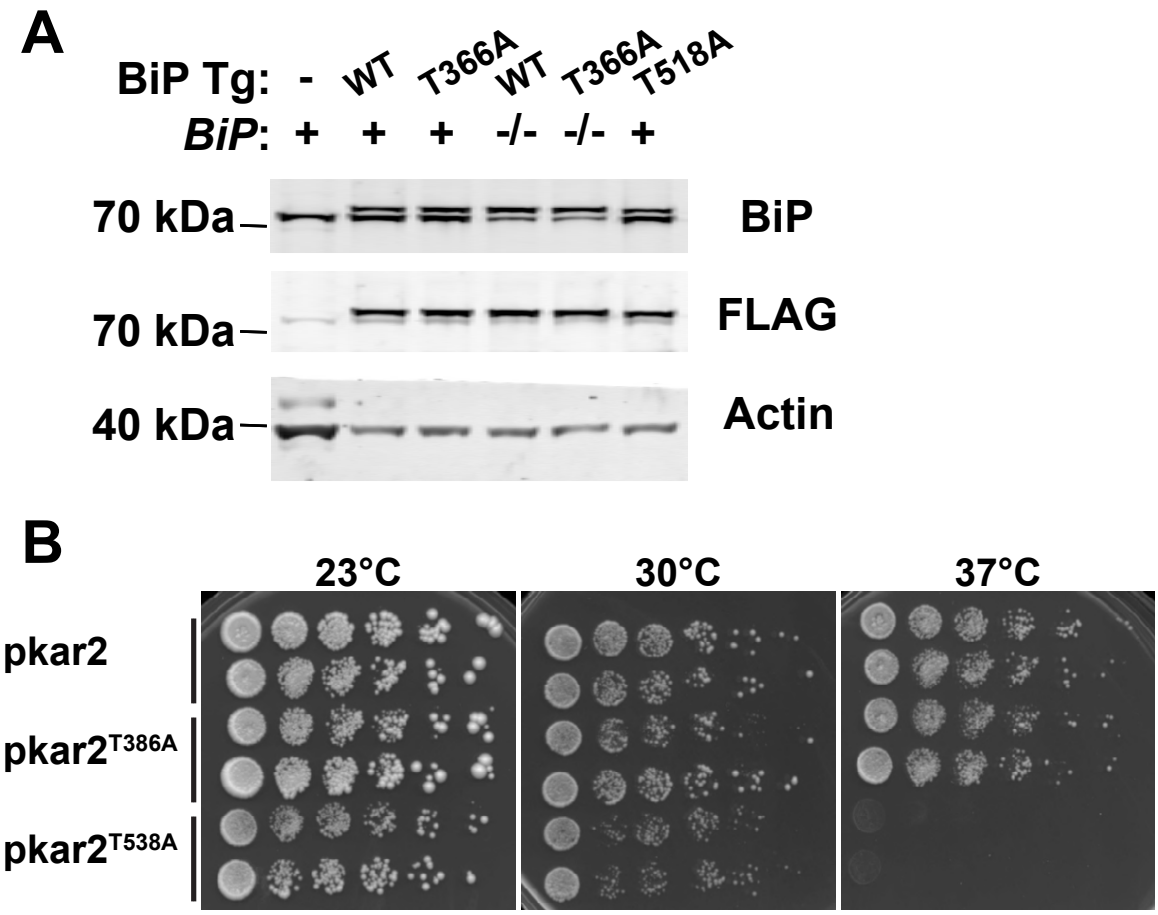

Figure 1- figure supplement 1. Expression of genomic BiP transgenes

(A) Western blots for FLAG-tagged BiP transgenes and total BiP in whole head lysates in *BiP* wild type or homozygous mutant background as indicated. Actin (JLA-20) served as a loading control. **(B)** Kar2^{T538A} mutants have temperature-sensitive growth defects. Yeast strains *kar2*Δ +p*Kar2*, *kar2*Δ +*pkar2*^{T386A}, and *kar2*Δ +*pkar2*^{T538A} were grown at 25°C and five-fold serially diluted onto plates of rich media incubated at the indicated temperatures.

bioRxiv preprint doi: https://doi.org/10.1101/348797; this version posted June 15, 2018. The copyright holder for this preprint (which was not certified by peer review) is the author/funder, who has granted bioRxiv a license to display the preprint in perpetuity. It is made available under aCC-BY 4.0 International license.

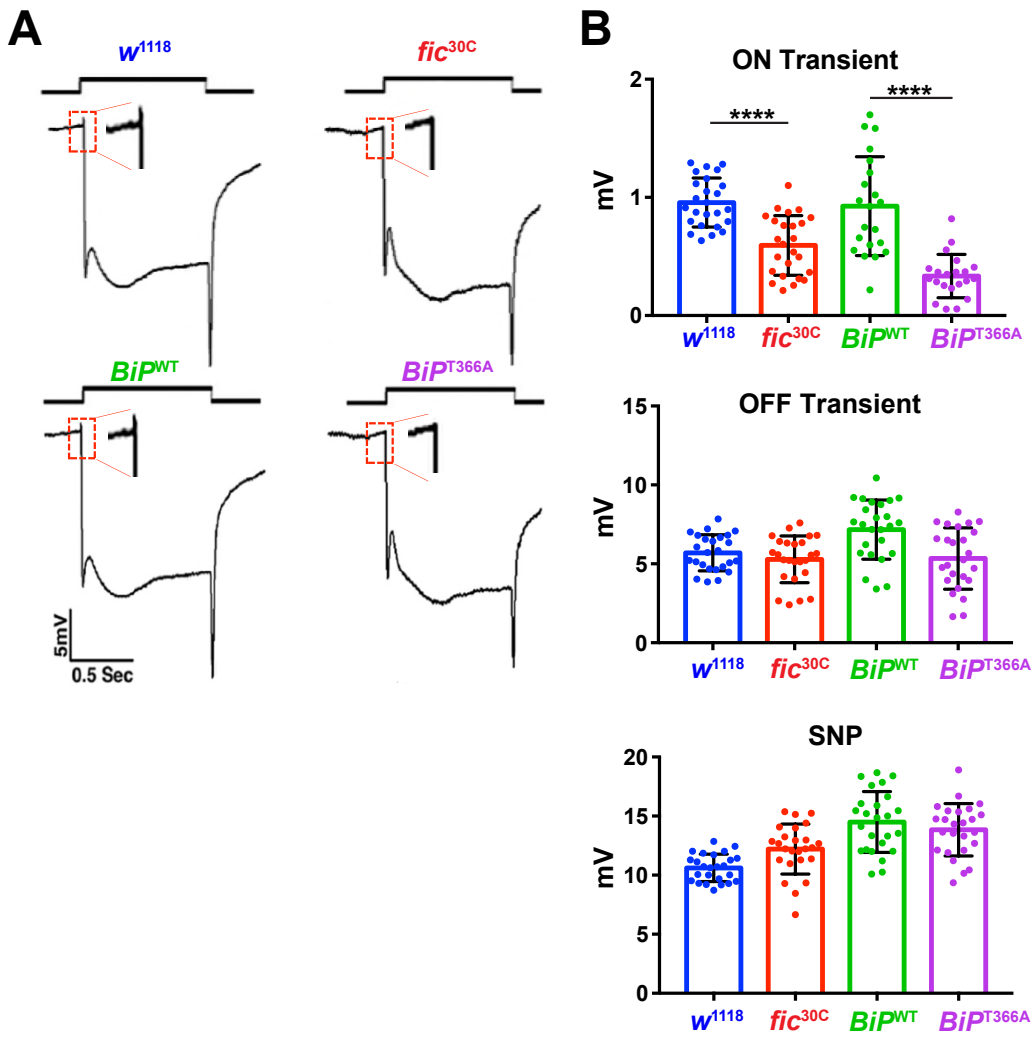

Figure 1- figure supplement 2. AMPylation-resistant *BiP*^{T366A} phenocopies *fic*.

(A) ERGs of *fic*^{30C} flies show reduced ON transients (arrows). Flies homozygous for a lethal *BiP*^{G0102} allele rescued by BiP^{WT} transgene have normal vision but flies rescued with the mutant BiP^{T366A} transgene display reduced ON transients. **(B)** Quantification of ERG traces. Bar graphs show means +/- SD. ****, $p < 0.0001$; ***, $p < 0.001$; *, $p < 0.05$; n= 24 flies per genotype and condition.

bioRxiv preprint doi: https://doi.org/10.1101/348797; this version posted June 15, 2018. The copyright holder for this preprint (which was not certified by peer review) is the author/funder, who has granted bioRxiv a license to display the preprint in perpetuity. It is made available under aCC-BY 4.0 International license.

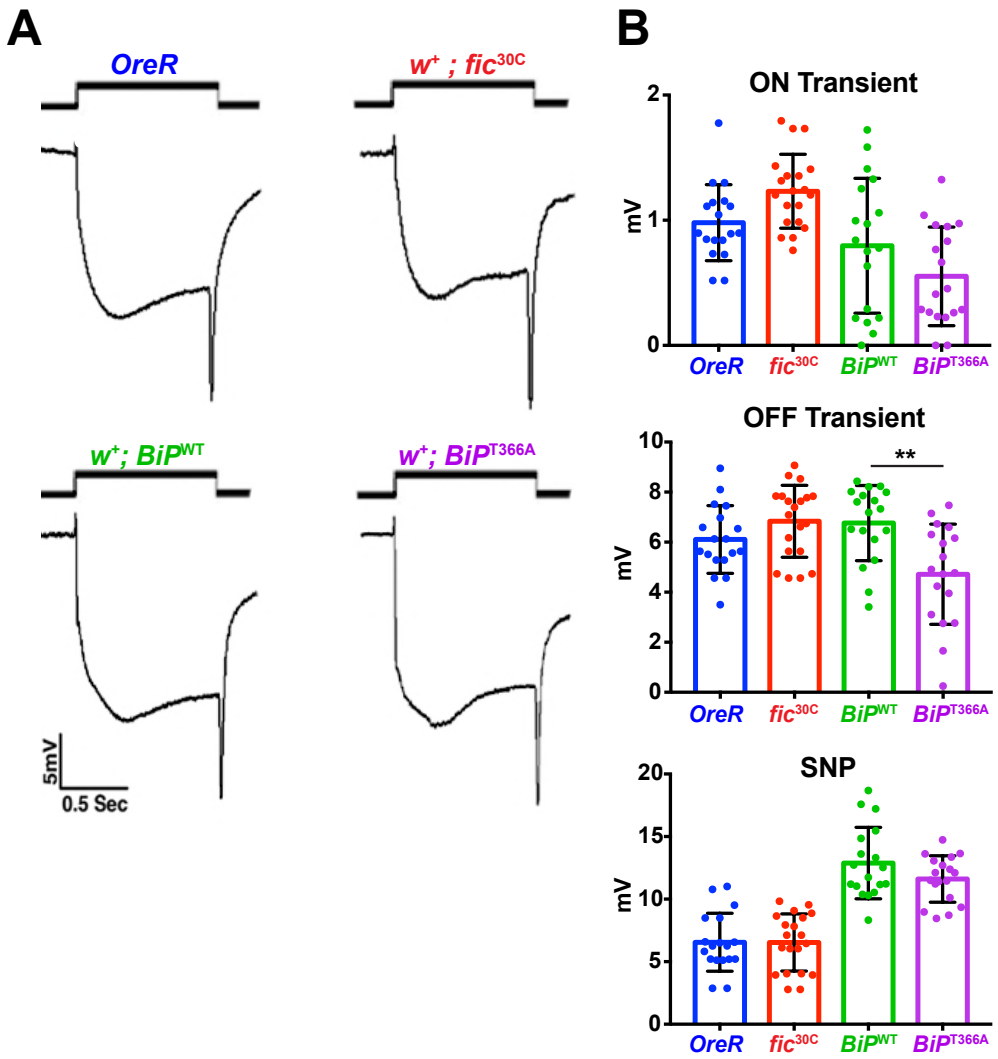

Figure 1- figure supplement 3. Red eye pigment suppresses ERG phenotypes of *fic*^{30C} and *BiP*^{T366A} mutants.

(A) ERGs of OreR and red-eyed *fic*^{30C} flies as well as BiP^{WT} and BiP^{T366A} animals. **(B)** Quantification of ERG data. Bar graphs show means +/- SD. **, $p < 0.01$, n= 18 flies per genotype and condition.

bioRxiv preprint doi: https://doi.org/10.1101/348797; this version posted June 15, 2018. The copyright holder for this preprint (which was not certified by peer review) is the author/funder, who has granted bioRxiv a license to display the preprint in perpetuity. It is made available under aCC-BY 4.0 International license.

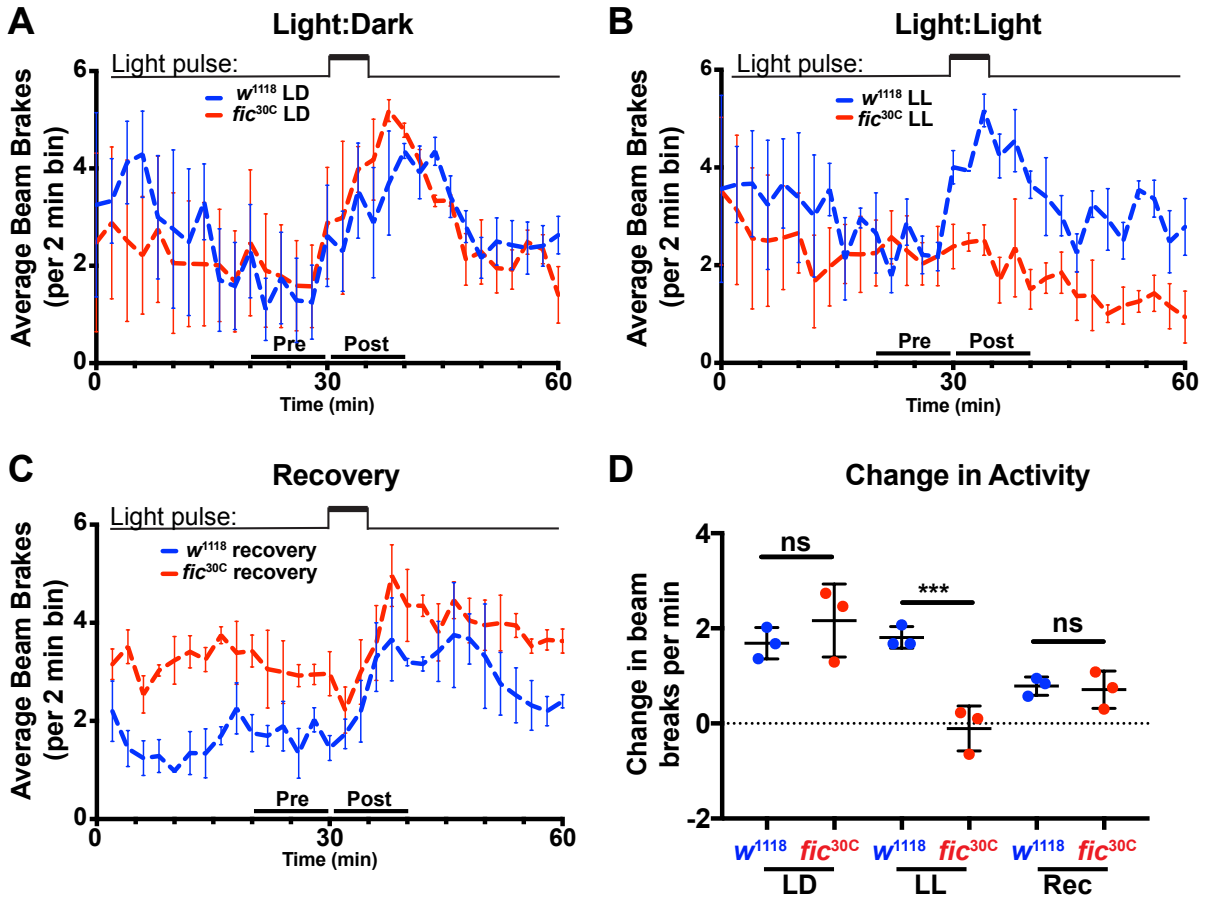

Figure 3- figure supplement 1. Light-induced defects in light-startle activity in *fic*^{30C} mutants.

(A, B, & C) Actogram of w^{1118} or *fic*^{30C} flies reared in LD for three days **(A),** LL for three days **(B)**, or recovery condition (three days in LL then three days in LD) **(C).** Light pulse is indicated by upper bars. Data is averaged from three biological replicas, each containing 16 flies per genotype. Data were collected in two-minute bins. Error bars represent Standard Error. **(D)** Quantification of change in beam breaks per 2-min bin for the 10 min intervals before and after the onset of the light pulse in each experiment. Bar graphs show means +/- SD. ***, $p < 0.01$, n= 3 experimental repeats with 16 flies per genotype and condition. Dead flies and those with a change in activity greater than 3 deviations from the median were excluded.

bioRxiv preprint doi: https://doi.org/10.1101/348797; this version posted June 15, 2018. The copyright holder for this preprint (which was not certified by peer review) is the author/funder, who has granted bioRxiv a license to display the preprint in perpetuity. It is made available under aCC-BY 4.0 International license.

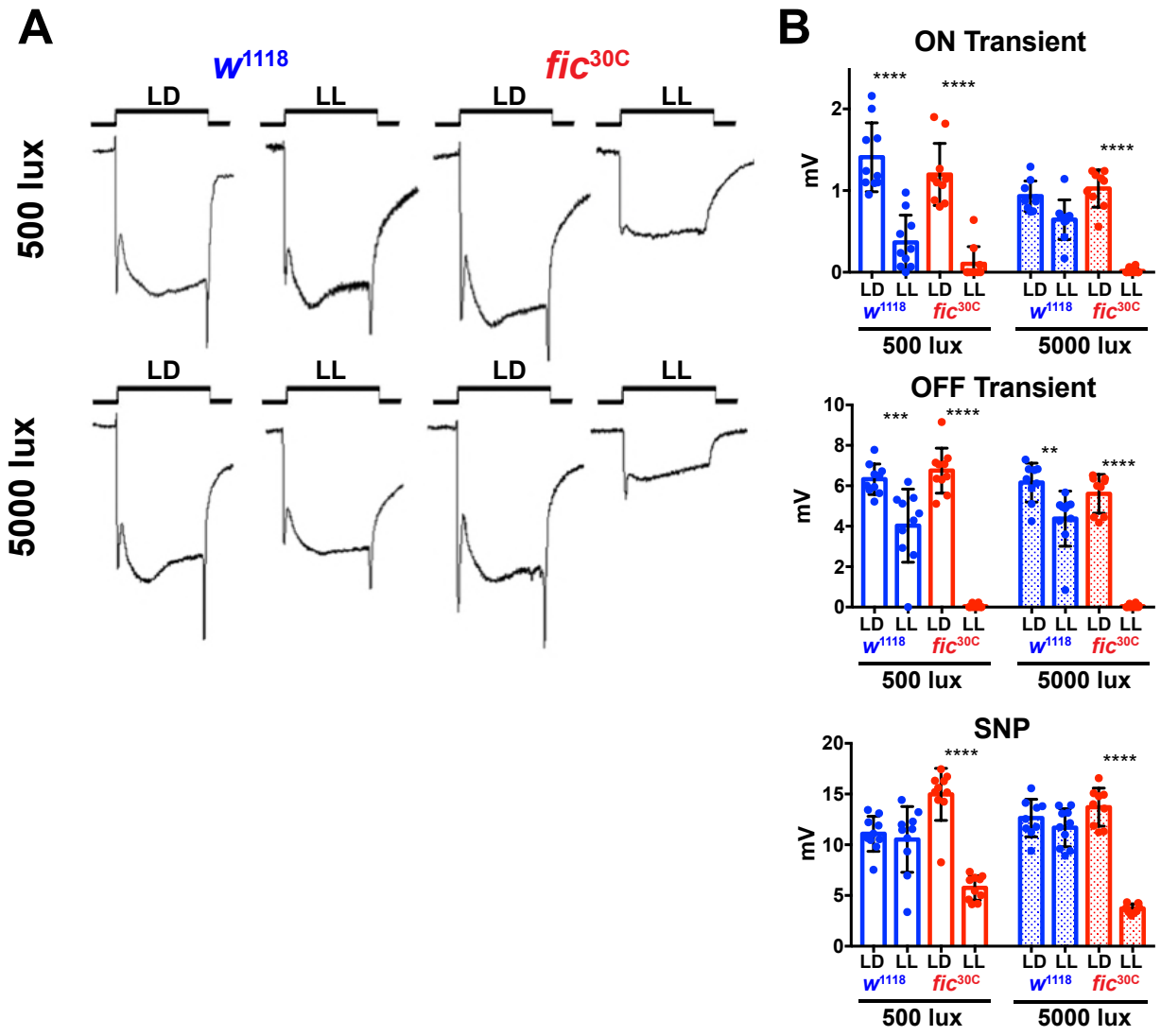

Figure 3- figure supplement 2. *fic*^{30C} mutants are sensitive to constant light, regardless of total intensity.

(A) Representative ERGs of flies following 3 days of LL or LD with either 500 lux or 5000 lux light, showing *fic*^{30C} null animals lose ON/OFF transients and have reduced SNPs with constant light, regardless of intensity, but under LD conditions, even at 5000 lux, have healthy ERG responses. **(B)** Quantification of ERG data. Bar graphs show means +/- SD. ****, $p < 0.0001$; ***, $p < 0.001$; *, $p < 0.05$; n= 10 flies per genotype and condition.

bioRxiv preprint doi: https://doi.org/10.1101/348797; this version posted June 15, 2018. The copyright holder for this preprint (which was not certified by peer review) is the author/funder, who has granted bioRxiv a license to display the preprint in perpetuity. It is made available under aCC-BY 4.0 International license.

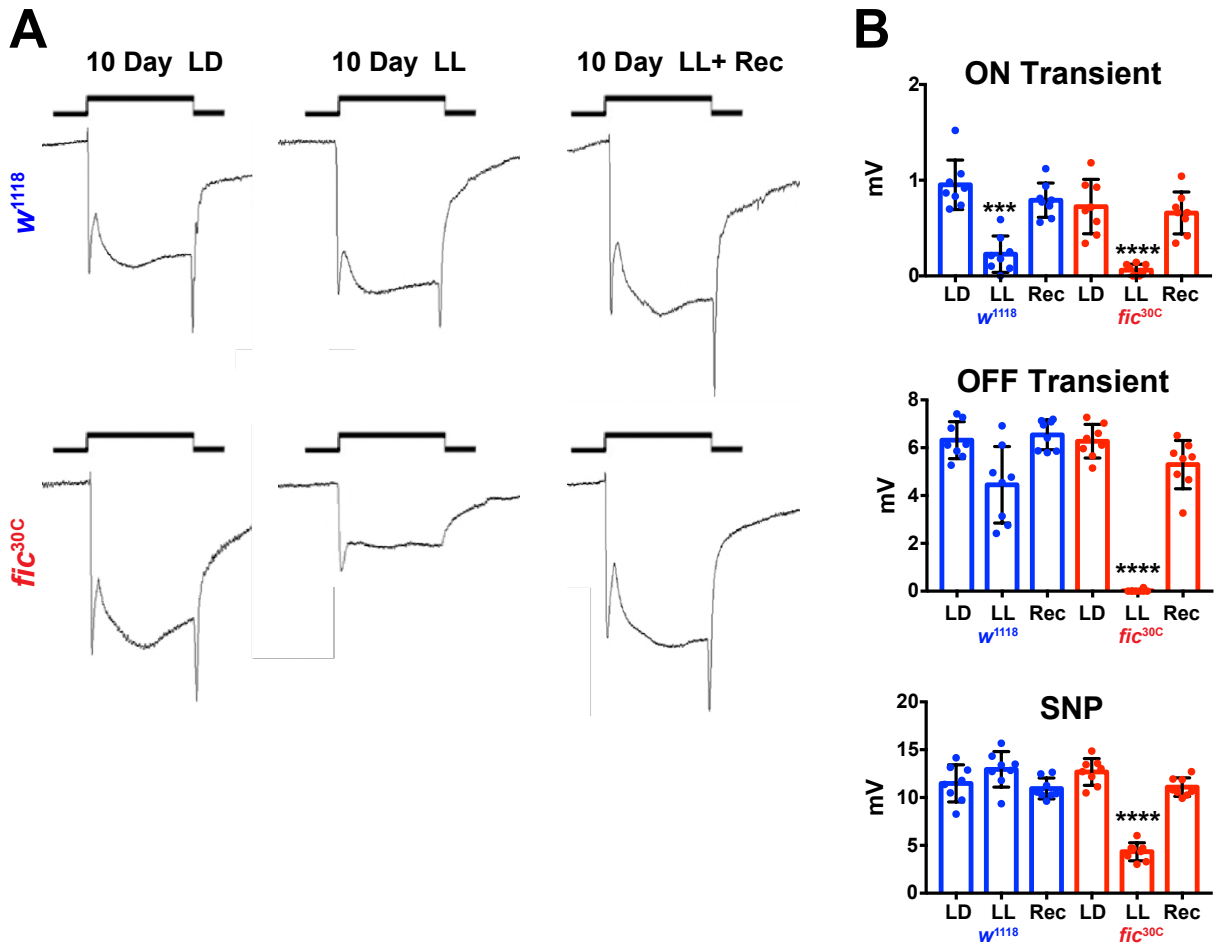

Figure 3- figure supplement 3. *Fic*^{30C} mutants recover ERG properties in 72 hours after 10 days of LL.

(A) Representative ERGs of flies following 10 days of LL, 10 days LD (500 lux), and 3 days Recovery following 10 days. **(B)** Quantification of ERG data. Bar graphs show means +/- SD. ****, $p < 0.0001$; ***, $p < 0.001$; *, $p < 0.05$; n= 8 flies per genotype and condition.

bioRxiv preprint doi: https://doi.org/10.1101/348797; this version posted June 15, 2018. The copyright holder for this preprint (which was not certified by peer review) is the author/funder, who has granted bioRxiv a license to display the preprint in perpetuity. It is made available under aCC-BY 4.0 International license.

Line	RNAi Target Gene	Eye Roughness Score					Weighted Average	Number of Flies	P-Value (Fisher's)
		0	1	2	3	4			
Control	***None***	0	1	68	3	0	2.03	72	n/a
BS36815	4EBP	0	0	96	0	0	2.00	96	0.032
v2935	ATF4	Lethal	Lethal	Lethal	Lethal	Lethal	Lethal	Lethal	Lethal
BS25985	ATF4	0	0	51	98	0	2.66	149	2.20E-16
BS26211	ATF6	0	2	68	2	0	2.00	72	1.000
BS64873	CaBP1	0	3	42	0	0	1.93	45	0.137
BS58172	Calnexin	0	2	41	1	0	1.98	44	0.688
v7799	eIF2a	0	2	54	0	0	1.96	56	0.302
v104562	eIF2a	0	0	48	0	0	2.00	48	0.388
BS55657	ergic53	0	5	35	7	0	2.04	47	0.007
BS35023	Gadd45	0	0	45	3	0	2.06	48	0.811
BS34346	GP93	0	0	33	5	0	2.13	38	0.122
v39561	Ire1	0	0	33	40	0	2.55	73	4.14E-12
v39562	Ire1	0	0	15	47	0	2.76	62	2.20E-16
BS62156	Ire1	0	0	0	57	2	3.03	59	2.20E-16
BS36743	Ire1	0	0	0	14	13	3.48	27	2.20E-16
BS28039	PDI	0	0	20	2	0	2.09	22	0.685
v110278	PERK	0	0	3	45	4	3.02	52	2.20E-16
v16427	PERK	0	0	0	13	30	3.70	43	2.20E-16
BS35162	PERK	0	0	28	43	0	2.61	71	6.84E-14
BS42499	PERK	0	0	26	65	50	3.17	141	2.20E-16
BS36755	Xbp1	Lethal	Lethal	Lethal	Lethal	Lethal	Lethal	Lethal	Lethal
BS25990	Xbp1	Lethal	Lethal	Lethal	Lethal	Lethal	Lethal	Lethal	Lethal

Table 1. Genetic interactions between Fic and UPR genes.

UAS^{Scer}-driven RNAi transgenes (either TRIP or VDRC lines) were used to silence candidate UPR and ER stress-related genes in a *fic*^{30C}/+ heterozygous background, with either *LongGMR*-Gal4, UAS-Fic^{E247G} or *LongGMR*-Gal4 only. Eye roughness was scored for individual flies and averaged for each cross. Table reports number of flies scored in each group (0=no roughness, 2=mildly rough (control flies), 4= severely rough, 1 and 3 are intermediate phenotypes) and the weighted average of the eye roughness. Significance differences are highlighted in yellow, and p-value's were determined using Fisher's Exact Test for categorical data, comparing the effects of each gene knockdown with the control group (**top line**, *fic*$^{30C/+}$; *LongGMR*-Gal4, UAS-Fic^{E247G}). Interactions were considered significant for any individual test if $p < 0.003$ as determined using Bonferroni's multiple comparison adjustment.